NASA CONTRACTOR REPORT

NASA CR-430

CALCULATION OF TWO-DIMENSIONAL TURBULENT FLOW FIELDS

by John G. Trulio, William E. Carr, William J. Niles, and Richard L. Rentfrow

Prepared under Contract No. NAS 8-11400 *by*
NORTHROP CORPORATION
Newbury Park, Calif.
for George C. Marshall Space Flight Center

NATIONAL AERONAUTICS AND SPACE ADMINISTRATION - WASHINGTON, D. C. - MAY 1966

CALCULATION OF TWO-DIMENSIONAL TURBULENT FLOW FIELDS

By John G. Trulio, William E. Carr, William J. Niles,
and Richard L. Rentfrow

Prepared under Contract No. NAS 8-11400 by
NORTHROP CORPORATION
Newbury Park, Calif.

for George C. Marshall Space Flight Center

NATIONAL AERONAUTICS AND SPACE ADMINISTRATION

For sale by the Clearinghouse for Federal Scientific and Technical Information
Springfield, Virginia 22151 – Price $1.25

ABSTRACT

Numerical solutions of the Navier-Stokes equations have been obtained for the flow of a compressible viscous fluid around a right circular cylinder. All planes normal to the cylinder axis are assumed to be planes of symmetry for the system. A computer code (called AFTON 2P) which solves the equations of motion of a general continuous medium for two-dimensional plane symmetric systems, was specialized to the case of a Stokesian fluid and used to solve these problems. Eulerian boundary conditions were developed for both subsonic and supersonic flow in a form suitable for numerical computation, and put into the code. The Mach number in all flows was 0.2. The Reynolds number R was varied over the range R = 100 to R = ∞ ; no data are presented here above a Reynolds number of 5000. Three different finite difference meshes were used to provide information on the effect of the mesh point density on the numerical solutions. At R = 100 and R = 1000, vortices formed in the wake of the cylinder in a manner similar to that observed experimentally. With R = 5000, a random-looking velocity field, rather than a vortex flow pattern, developed in the wake of the cylinder - again in qualitative agreement with experiment.

The system with R = 100, which was otherwise symmetric about a plane through the cylinder axis, was perturbed asymmetrically in order to induce vortex shedding. A vortex street developed with a shedding frequency within 10 percent of that measured experimentally.

Using our finest mesh, the code predicted sizable pressure fluctuations for R = 1000 in the neighborhood of the cylinder, at a dominant frequency of about 50 kilocycles. It is not clear yet whether these fluctuations are physically real, or a quirk of the numerical method. With sufficiently coarse meshes or appropriate time averages, the pressures calculated at various points of the cylinder were in fair agreement with those measured. Graphs of the pressure as a function of the cylinder angle θ are presented, as are many plots of the velocity fields obtained in the calculations.

TABLE OF CONTENTS

Acknowledgments

The authors are pleased to acknowledge the many helpful suggestions and discussions provided in the course of this work by the staff of the Unsteady Aerodynamics Branch of the Marshall Space Flight Center's Astro-Aerodynamics Division. The encouragement and keen interest of Mr. Thomas Reed, Mr. Gilbert Wilhold, Dr. Max Platzer, Dr. Richard Rechtien and Mr. Luke Schutzenhofer have been especially gratifying.

The computer code used to generate the flow fields which are the principal results of the work reported here is a modified version of a more general code developed under Air Force Contract AF 29(601)-5971 for the prediction of the ground motions induced by nuclear explosions. The work of Contract AF 29(601)-5971, funded by the Defense Atomic Support Agency as part of the Project FERRIS WHEEL, is being continued under Contract AF 29(601)-6683.

1.0 INTRODUCTION

1.1 Objectives and Summary of Major Results

The overall objective of this program was to determine the feasibility of solving the equations of motion of a viscous compressible fluid for systems of practical interest by recently developed numerical techniques. To attack such problems numerically, the continuous variables of space and time are replaced by a finite discrete mesh of points. As the density of points in the mesh is increased, it more and more closely approximates the space-time continuum, at least in the sense that any piecewise continuous function can be represented more and more accurately by specifying its discrete values at the mesh points. It also appears that finite difference equations can be written whose solutions approach those of the equations of motion of the continuous medium in the same sense - as the mesh point density is increased, the discrete values of the flow variables, found at the mesh points from the finite difference equations, more and more closely approximate an exact solution of the equations of motion. No formal proof of this statement can be given, but it is strongly suggested by general experience over the last twenty years - approximately the span of time in which finite difference methods have been used extensively to solve continuum motion problems. Of course, it is also true that the cost of solution of a given problem increases when the density

of discrete mesh points is increased. Hence, the question of the feasibility of these methods for viscous compressible flow problems ultimately becomes an economic one - can such problems be solved cheaply enough to make the method practical? To a lesser extent, feasibility is also a question of how long a compute must be run to solve such a problem. However, the cost, speed and reliability of presently available computers are such that in deciding whether a numerical technique is useful, cost considerations usually overwhelm such factors as the length of computing time needed, or the possibility of machine error.

Numerical methods developed earlier by the people active in this program were made the basis for all the calculations of the program.[1-4] As a test of these methods, attention was focussed on the problem of compressible viscous fluid flow around an infinite right circular cylinder. It was assumed that the Navier-Stokes equations governed the flow of the fluid while a polytropic gas equation of state determined its pressure. This case was chosen for two reasons. First, prior to the start of this program, a computer code had been developed to describe the plane symmetric flow of a general continuous medium.[4] Secondly, this particular viscous flow problem seems to have been studied experimentally more thoroughly than any other, so that it offers the

possibility of a relatively good check on the numerical results. In the course of the program, flow fields were calculated numerically for several Reynolds numbers from 100 to infinity, a range of values which includes the formation of vortex streets and turbulent wakes, and the transition between them. By comparing the results of these calculations with measured results, one can get a general idea of the accuracy of the numerical method for problems of this kind. A basis for comparison between experiment and numerical theory is found in such flow characteristics as the stress on the cylinder at various points, the appearance and position of a point of separation of a flow, and the frequency of shedding of vortices.

Similar calculations for incompressible fluid flow have been made by other investigators, with very impressive results.[5,6] It is important to distinguish the methods used in this program from those employed to solve incompressible fluid flow problems. In that case, the fact that the flow is divergenceless is essential to the formulation of the differential equations whose solution is to be effected numerically. The techniques used in this program are free of this restriction; they apply to the general motions of continuous media in two-dimensional plane geometry, rather than to the smaller class of incompressible flow problems. In fact,

incompressible flow can only be approached as a limiting case by the methods used here. The reason for this is that the numerical solution of a flow problem proceeds in finite time-steps whose size is inversely proportional to the sound speed in some part of the flow field. Since the speed of sound is infinite for an incompressible fluid, the calculation would have to be made with infinitesimal time-steps, and would require infinite computing time on a digital computer.

To some extent, the results presented here show that the numerical methods used to obtain them provide a practical approach to the solution of general viscous compressible fluid flow problems; to what extent, is at least partly a subjective matter. On the whole, it seems fair to claim that these numerical methods are of practical significance now, and will probably constitute an important theoretical tool for the study of turbulence (and viscous fluid flow phenomena in general) in the future. While the method cannot be endorsed without reservation on the basis of the work of this program, it has so far been quite successful in most respects. First, at a Reynolds number of 100, sufficiently extensive calculations were made to allow the shedding of several vortices and the formation of a clearly defined vortex street. Next, it was found possible to describe qualitatively the formation of vortices in the range of Reynolds numbers from 100 to 1000.

Further, it was found that at a Reynolds number of 5000, no vortex formation took place at all, but only something resembling the formation of a turbulent wake. This is in agreement with experimental observation; between a Reynolds number of 1000 and 5000 the flow field for some reason changes its character drastically in this way.[7] It was hoped that some light could be shed on the reason for the transition. In this connection, the numerical results for a Reynolds number of 100 indicated an aspect of the flow field behavior which may be important in the formation of turbulent wakes. In analyzing the pressure at various positions on the cylinder, it was found that as the mesh was refined, the pressure field tended to have a random spatial variation. As a function of time, the pressure appeared, on closer inspection, to undergo roughly periodic oscillations whose amplitude was a sizeable fraction of the pressure head. Each of the points studied at the back side of the cylinder showed generally this same kind of pressure-time fluctuation. However, all of the pressure-time curves were out of phase, so that at any given instant the pressure field appeared to be spatially random. At a Reynolds number of 1000, the period of these oscillations was found to be about 20 microseconds; no study has been made yet to determine whether the mean period varies with Reynolds number. At lower Reynolds numbers, i.e., for fluids of greater viscosity, the pressure fluctuations were reduced in amplitude, owing to the

damping effect of the viscous forces. At a Reynolds number of 1000, these fluctuations are large; with a further reduction in viscosity, they would most likely become even larger and might dominate the flow entirely. The computer code results suggest that this is indeed what happens when vortex formation passes over into turbulent flow with increasing Reynolds number. Where coarser meshes are used, or if the pressures obtained with fine meshes are averaged over a suitably long time interval, then the calculated pressures agree more closely with available experimenta data. However, there is at least one respect in which the numeric results obtained so far are not satisfactory. The region occupied by the vortex street appears to be more constricted near the cylindrical obstacle than experimental streamline flow patterns indicate; the vortices are narrower than they should be, and appear to be elongated in the direction of the free stream flow. Nevertheless, the frequency of shedding of vortices at a Reynolds number of 100 (the only case tested in this respect) agrees well, i.e., to within ten per cent, with the value found experimentally. On the whole, the results obtained in this program might reasonably be said to establish these numerical methods as a practical design tool of considerable promise for a much larger class of viscous compressible fluid systems than has heretofore been mathematically tractable.

1.2 Economic Limitations of the Numerical Method

There are two general approaches to the numerical solution of the equations of motion of a continuous medium. These can be classified as time-marching methods and characteristic methods. Time-marching methods make explicit use of time as an independent variable in accord with the most elementary and basic statements of the underlying principles of classical mechanics.[1-4,8] On the other hand, characteristic methods, which treat continuum motion as a problem in wave propagation, make use of the envelopes of sound signals in space-time as coordinate surfaces.[9] The numerical technique used here, and the computer codes based on it, are of the time-marching kind. Numerical methods of this kind share an important common restriction on the accuracy of the numerical solutions which they provide.[4] The values of the variables of the motion at the points of the finite difference mesh can, and hopefully do, converge toward values of an exact solution of the equations of continuum motion as the density of mesh points is increased. However, the rate of convergence is sharply limited as a function of a typical or mean mesh spacing parameter h; the error in the finite difference solution, as compared to the exact solution, cannot be made to tend to zero more rapidly than $h^{3/2}$.[4] The reason for this restriction lies ultimately in the finite speed of sound

in real materials. Since disturbances require a finite time to propagate over finite distances, quite different physical states can coexist in the same finite region. For example, one part of a gas column can find itself in a uniformly quiet state, while another part of the same column of gas is in motion. As a result, in almost all continuum motion problems of interest, space-time is divided into finite regions by surfaces across which some derivatives of the flow variables with respect to position or time experience a jump discontinuity. Moreover, these derivatives are typically of low order, and most often are first derivatives. Time-marching numerical schemes of solution of continuum motion problems must entail the evaluation of terms which tend to the partial derivatives appearing in the equations of motion in differential form. Schemes which are formally of high accuracy (in the sense that the error in the numerical solutions which they yield tends to zero as some high power of the mesh spacing) actually achieve these rates of convergence only if corresponding high-order derivatives are continuous everywhere on the region of space-time germane to the flow. Since second derivatives of the variables of the motion with respect to space or time coordinates generally have infinite discontinuities somewhere on the flow region the rate of convergence should not be expected to be as rapid as the second power of the mesh spacing parameter. On the other hand,

the region of space-time on which the difference equations are necessarily a poor approximation to the governing differential equations is confined to the neighborhood of isolated surfaces in space-time, while the flow takes place throughout a volume of space-time. Hence, the error in the solution should be expected to vanish at least as rapidly as the first power of the mesh spacing. More detailed investigation of the finite difference equations of Richtmyer and von Neumann,[8] which are among the simplest and most successful of time-marching schemes, has led to the conclusion, stated earlier, that the numerical solution error will tend to zero as the 3/2 power of the mesh spacing parameter.[4] This law of decay has some important economic implications. In one space dimension, the time of solution, and hence the cost of a problem, is nearly proportional to n^2, where n is the number of mesh points representing a continuous spatial coordinate. In two dimensions it is proportional to n^3, and in three dimensions, to n^4. Hence, if the truncation error is proportional to $h^{3/2}$, as it appears to be for time-marching schemes employing centered differencing, then to cut the solution error by a factor of 2 will increase the cost of solution by a factor of 2.5 in one dimension, 4 in two dimensions, and 6.3 in three dimensions. If the truncation error is proportional to h^2, which is possible in principle for centered differencing of the equations of motion in characteristic

form, then the factors are 2, 2.8, and 4.

General experience in the use of these techniques has shown that for one-dimensional flows it is usually necessary to employ on the order of a few hundred mesh points - say 200 - to obtain quantitatively satisfactory results. It is unlikely that results of comparable accuracy will be obtained in two space dimensions unless the square of this number of mesh points is employed, and, in three dimensions, the cube of this number. Also, typically, the number of time-steps required to complete a problem of motion is on the order of a few thousand - say 2000. Thus, in the course of a nominal problem, the variables of the motion must be updated about $10(200)^{D+1}$ times to generate the solution to the problem, where D = 1, 2, 3 for motion in one, two, and three spatial dimensions, respectively. If one considers that the time of solution of a problem on a high speed computer should not be greater than about 10 hours, then the computer on which the calculations are performed must be capable of updating the variables of one-dimensional motion at one space point by one time-step in about .045 seconds. Computers which meet this requirement have been available for a number of years. For two-dimensional problems, an adequate computer would have to update the variables of the motion at one space point by one time-step in about 200 micro-seconds. Computers approaching this capability have only recently

become available. In all but a few special cases, three-dimensional problems are well beyond the state-of-the-art of present-day computer development.

The problems of interest in this program are two-dimensional, and lie at about the limit of the power of present computers. It is for this reason that the program was essentially a feasibility study whose purpose was to determine the accuracy which could be realized in the solution of continuum motion problems by time-marching methods, using presently available computing machines for reasonable lengths of computing time. The 3/2-power decay law for the numerical solution error implies that once a good distribution of mesh points has been found for a given problem, greater accuracy can only be had by increasing the mesh point density; as the solution error is decreased in this way, the rule also implies a rapid increase in the cost of solution. Computing speed appears to be the only answer to this law; for the problem-solver whose specific continuum motion problem is not of a kind routinely solved, the adequacy of available computers for his purpose is likely to be decisive with respect to the use of numerical methods for many years to come.

2.0 COMPUTER CODE INPUT AND OUTPUT FOR THE CALCULATIONS

2.1 Parameters of the Flow Field Calculations

Numerical methods for the solution of physical problems generally involve two kinds of parameters, namely, physical parameters and mathematical parameters. The physical parameters characterizing systems of the kind considered in this program consist of the Reynolds number, Mach number, heat capacity ratio for the gas, and the shape of the rigid obstacle in the flow field. The principal mathematical parameters are the positions selected for the points of the finite difference mesh used to describe the flow - the so-called "zoning" parameters of the flow field. The time-step is also variable, within limits set by considerations of numerical stability;[8,10] roughly, in these problems, the time-step was so chosen that a sound signal would require two time-steps to traverse the shortest distance across any zone of the mesh. Other mathematical parameters enter the numerical calculation in that numerical results can be generated in practice only for a finite flow region, while in the first instance the flows of interest here take place in an infinite plane field. Thus, a closed curve must be chosen to bound the portion of the flow region on which the history of the flow is to be calculated; this choice is left to the intuition or previous experience of the problem-solver. Finally, the precise finite difference representation of the boundary conditions

used to describe the flow, as well as the finite difference equations of motion, are also to a large extent at the discretion of the problem-solver - although it would be inaccurate to classify them as parameters. A discussion of the boundary conditions will be given later in this report. As a guide to writing appropriate difference equations, the requirement has been imposed that these equations satisfy certain important transformation conditions. For example, the differential equations for conservation of mass and momentum, taken with the first law of thermodynamics, imply a conservation equation for the total energy. The difference analogs of the mass, momentum and first law equations used in this program rigorously imply a difference analog of the total energy equation which is also exactly conservative. Moreover, the difference equations have been written to satisfy this criterion in a general time dependent coordinate system. The finite difference technique, and its rationale, are discussed in more detail elsewhere.[1-4]

Ideally, only the physical parameters of a problem would determine the outcome of a numerical computation, just as only these parameters affect what happens in nature. However, although practical interest in a numerical method centers on its physical parameters, it is necessary also to know how the mathematical parameters influence computed output, if the results of numerical computation are to be understood. Accordingly,

much of the work of the program dealt with the influence of the mathematical parameters of the numerical method. In fact, the numerical work of the program consisted largely of a variation of mesh spacing parameters and of the Reynolds number.

2.2 Input to the Specific Calculations of the Program

The obstacle in the flow field was taken in every case either as a perfect right circular cylinder or as a slightly flattened one. All the calculations were made in a frame of reference in which the cylinder was stationary; the positions of the mesh points were specified in Cartesian x, y form referred to the center of the cylinder as the origin of coordinates. In addition, the mesh point positions were held fixed throughout any problem. The meshes used here are therefore Eulerian. They are also logically rectangular, in the sense that the points of any finite difference mesh can be labelled by a pair of integers j, k, where x increases as j increases and y increases as k increases. However, the points comprising any given mesh are not arranged in straight lines, i.e., the mesh points define zones which are quadrilaterals, but not necessarily rectangles, in the x, y plane. The reason for this is that the obstacle itself is not rectangular and most naturally calls for a non-rectangular coordinate system to describe the flow field in its vicinity. The free stream flow direction was taken to be the direction of the y-axis; the x-axis is therefore at right angles to the direction of free stream flow. The points for which j has its minimum value, and the points for which j is a

maximum, define two lines of constant x; these lines will be called the "lateral boundaries" of the region of calculation of the flow. The points for which k has its minimum value lie on a line of constant y, called the "upstream boundary" of the flow region; the points for which k has its maximum value also define a line of constant y, called the "downstream boundary" of the region of calculation of the flow. Thus, each flow field was calculated on a finite rectangular region of the x, y plane.

In all the code runs, the diameter of the cylinder was taken to be three units of distance, and one of the lateral boundaries of the region of calculation of the flow was the line $x = 10$. The other lateral boundary was either the y-axis itself or the line $x = -10$, depending on the symmetry of the flow field. That is, the y-axis was a line of reflective symmetry for the flow field in some of our calculations, particularly in the first half of the program. A flow begun with perfectly symmetric initial conditions and subject to perfectly symmetric boundary conditions maintains its symmetry, although such flows are unstable with respect to symmetry perturbations and are therefore not observed in nature. For such symmetric flows, the flow field need only be calculated on one side of the line of symmetry; the amount of computation is halved thereby. It was for this case that one of the lateral boundaries was the line $x = o$, while for problems lacking reflective

symmetry the corresponding lateral boundary was the line x = -10. The upstream boundary was the line y = -6.75 in all cases. The downstream boundary was taken as the line y = 9, except for the last (and lengthiest)code run, in which the downstream boundary was the line y = 15.

Three different finite difference meshes were used in the program. They will subsequently be called "fine", "medium", and "coarse", these terms corresponding to the order of decreasing density of mesh points. With the lines x = ± 10, y = -6.75 and y = 9 bounding the region of calculation of the flow, the fine, medium and coarse meshes consisted of logically rectangular arrays of 59 x 59, 43 x 48, and 29 x 29 mesh points, respectively, except that the centerline of the problem bifurcates to define the cylinder. However, the fine mesh was actually used only for the case in which the y-axis was a line of reflective symmetry of the flow; fine mesh calculations were therefore made only for a grid of 30 x 59 mesh points. Figures 1, 2, and 3 show the plane two-dimensional arrays of points making up the three meshes.

In all the work of the program, the air pressure was taken as that of a polytropic gas with a heat capacity ratio of 1.4. Also, changes in the state of any air mass element were assumed to take place adiabatically; owing to the viscous forces represented by the deviatoric stresses in a Stokesian fluid, changes

in the entropy of any mass element are possible in subsonic flow, and were allowed to take place in the numerical calculations. A Mach number of .2 was used almost exclusively in these calculations The only exception is to be found in some of our first code runs, which employed very coarse finite difference meshes, and were carried out for debugging purposes; no further reference will be made to these calculations. In all cases the variables of the motion at the upstream boundary were given their free stream values. A no-slip condition was applied at the surface of the obstacle, while a condition of frictionless sliding was imposed at the lateral boundaries. The downstream boundary was treated in two different ways. Most of our numerical work was done with a very crude description of this boundary, in which the variables of the motion were assumed to have the same values at the boundary itself as at the immediately adjacent interior mesh points and zone centers. In our most recent code runs, the downstream boundary was handled in a more sophisticated way; as described in the next section, the new downstream boundary calculation is based on the treatment of streamlines as regions of one-dimensional slab flow in the neighborhood of the boundary.

A stationary cylinder surrounded by air at standard conditions, moving uniformly in the direction of the positive y axis at Mach .2, comprised the basic set of initial conditions for the

TABLE I

Summary of Problems Run

PROBLEM NUMBER	REYNOLDS NUMBER	MESH*	X RANGE	Y RANGE	TIME STEP	NUMBER OF CYCLES RUN
SYMMETRIC CASES						
108.2	1000	C	0,10	-6.5,8	.00175	800
110	∞	C	0,10	-6.5,8	.00175	100
112.1	1000	F	0,10	-6.75,9	.00058333	1200
112.1	1000	F	0,10	-6.75,9	.00029167	400-600
113	10000	C	0,10	-6.5,8	.00175	300
NON-SYMMETRIC CASES						
208	1000	C	-10,10	-6.5,8	.002625	1700
208.1	1000	C	-10,10	-6.5,8	.00175	1700
209	1000	M	-10,10	-6.75,9	.00175	2700
210	∞	C	-10,10	-6.5,8	.002625	700
211	10000	M	-10,10	-6.75,9	.00175	1000
211.1	1000	M	-10,10	-6.75,9	.00175	600-1000
211.2	5000	M	-10,10	-6.75,9	.00175	1200
211.4	100	M	-10,10	-6.75,9	.00175	950-2100
211.41	100	M	-10,10	-6.75,15	.00175	1900-4100
211.42	100	M	-10,10	-6.75,15	.00175	3900-4300
211.6	∞	M	-10,10	-6.75,15	.00175	1197
213	10000	C	-10,10	-6.5,8	.002625	700

* F = fine mesh, M = medium mesh, C = coarse mesh

calculations of the program. These are "impulsive" initial conditions in that relative to the air at (say) the upstream boundary, all the air is at rest, while the cylinder has an instantaneous speed of Mach .2. Not all flows were actually begun in this way; to save computing time some problems were initiated with output generated in other problems - but these in turn could be traced back to an impulsive start.

The values of the mathematical parameters and the Reynolds number which define each of the problems run in this program are given in Table 1.

2.3 Output Format and Examples of Plots

Computed results were obtained at first exclusively in the form of tables of edited output. For each mesh point or zone center (whichever is appropriate) the mesh point coordinates, momentum vector, velocity vector, density, specific internal energy, stress components and mass were among the variables tabulated. As the program progressed, various plots of flow field quantities were made, at first by hand, and later on standard digital plotters. These plots - particularly plots of the velocity field at various instants of time in the course of a flow - now constitute the chief mode of display of the calculated results. The velocity vectors are shown in the customary way as arrows whose length is proportional to their magnitudes. In the finite difference scheme employed here, velocity fields are computed at mesh points. Accordingly, in the flow field plots each mesh point is used as an origin for the velocity vector associated with that point. Many such plots have been made in the course of the program. Samples of these are given in Figures 4 - 8. In these plots, as in all the velocity plots shown in this report, the data exhibited is exactly that given by the finite difference equations; there has been neither smoothing of raw output, nor interpolation in the flow field. The coarse and medium meshes were used to describe both flows for which the

y-axis is a line of perfect reflective symmetry and flows for which it is not. It can be seen in a general way from the Figures that the computed output agrees with the observed patterns of flow for these systems.[11] In the fine mesh plots, the development and growth of one of the two perfectly symmetrical vortices at the back side of the cylinder is clearly shown, as is the motion of the point of separation of the flow from the backside of the cylinder to a position near its middle. In this case, with a Reynolds number of 1000, the number and distribution of mesh points were chosen largely to provide boundary layer detail. With a Reynolds number of 1000 the boundary layer is about three zones thick for the fine mesh, whereas it lies entirely within the one zone adjacent to the obstacle for the medium sized mesh, and in a fraction of this zone for the coarse mesh. It is interesting, and perhaps of practical importance, that it does not appear necessary to describe the details of boundary layer motion in order to obtain a picture of the flow which is at least qualitatively correct. A complete set of flow field plots generated in the program is in the possession of Marshall Space Flight Center personnel.

3.0 RESULTS OBTAINED IN THE PROGRAM

3.1 Principal Classes of Results

The main results of the program lie in four areas. With regard to the numerical method and its application, important information has been obtained concerning the effects of different choices of a finite difference mesh on the numerical output computed for problems of this kind; also, for the difficult subsonic case, a method has been developed for the treatment of boundaries which is physically reasonable in principle, which has now given physically reasonable output in practice, and which is capable of further refinement and generalization. Finally, two important comparisons have been made with experimental data; quantitative agreement has been achieved which is as close as one might hope to reach in this early stage of the application of the numerical method. One such comparison has to do with the frequency of shedding of vortices and with the transition to turbulence with increasing Reynolds number, while the other concerns the pressure on the downstream side of the cylinder and the mechanism of turbulent flow field formation. On the last point, the calculations predict pressure oscillations in the neighborhood of the cylinder which, if their physical reality is upheld in future studies, are a flow phenomenon not previously calculated theoretically, and perhaps connected in an essential way with the occurrence of a turbulent wake as opposed to a vortex street.

3.2 Mesh Point Density Variations

The effect of the mesh point density on the numerical solutions is evident in Figures 6 - 8 which show the velocity field near the downstream side of the cylinder all at the same early, transient stage of formation of the initial vortex in a symmetrical flow field at a Reynolds number of 1000. The formation of vortices is apparent in all three cases. However, it is also apparent from Figures 6 - 8 that the vortices obtained with the coarse mesh diffuse rapidly relative to the other two meshes. The results for the medium mesh show vortex growth as a smoothly continuous transformation of the velocity field. With the further definition afforded by the fine mesh, whirlpools and eddies can be seen on regions small compared to that occupied by the main vortex. It appears that similar phenomena occur in real physical flows.[12]

The average density of mesh points in the medium mesh is slightly more than twice that in the coarse mesh, while the fine mesh contains about four times as many points per unit area as the coarse mesh. In the neighborhood of the cylinder these ratios have deliberately been made somewhat larger to afford greater relative definition of the boundary layer in passing from the coarse, to the medium, to the fine mesh. By comparison with pictures taken experimentally for similar physical conditions,[11]

it is apparent that one cannot expect to obtain more than qualitative information from meshes whose point density is similar to that of our coarse mesh. For the medium and fine meshes it appears from these results that the numerical solutions will be quantitively useful. The inadequacy of the coarse mesh is pointed up even more strongly by Figures 9 - 14 which show the velocity field calculated with the coarse mesh, and with the medium mesh, respectively, for a Reynolds number of 100. In both cases the fields are shown a short time after the shedding of the first vortex. In the case of the coarse mesh, the detached vortex has already diffused to the point where it is no longer clearly discernible as a whirlpool, but appears rather as a region of rapid change of the velocity field. On the other hand, Figure 14 for the medium mesh shows a well-defined vortex, detached from the cylinder and travelling downstream with its integrity essentially unimpaired.

3.3 Upstream and Downstream Boundary Conditions

In all the work of the program, the density and velocity of material at the upstream boundary, and the internal energy density there, were given their free stream values. The downstream boundary conditions used in all the problems except the last amount essentially to the assumption that the velocity, density and internal energy density fields do not vary with position in the neighborhood of this boundary. While this might be an adequate assumption far downstream, it amounts to a non-physical constraint on the flow, news of which travels upstream under these subsonic conditions and eventually seriously interferes with the flow field (see Figures 15,16). This strong non-physical perturbation was tolerated until late in the program since most of our studies required only the calculation of flow fields in their transient early stages, before the downstream boundary could communicate with the cylindrical obstacle. About all that is required of a boundary calculation for this purpose is numerical stability; spurious signals generated at the boundary cannot influence the flow early in the process of vortex formation. However, when it became necessary to approach the periodic state as a limit of the transient flow, it was evident on the basis of results like those of Figure 16 that the downstream boundary conditions would have to be improved. The crude boundary conditions first used were replaced by a calculation based on two principal assumptions, namely,

that each streamline of the flow field in the neighborhood of the boundary at any instant of time constitutes a region of transient isentropic one-dimensional slab flow, and that the sound speed has its free stream value at the downstream boundary. The variables of the motion can then be calculated at the boundary as follows.

First, knowing the velocity field at an instant of time, the position of any particle can be updated by one time-step from an "earlier time" to a "later time". In particular, a particle position can be found at the earlier time such that one time-step later the particle will arrive at a given boundary mesh point. For this purpose the discrete velocity field is assumed constant during the time-step and is made spatially continuous by interpolation; we interpolated linearly. Thus, one can calculate the direction of the streamline along which that particle travels which arrives at the given boundary point at the later time. Assuming that sound signals travel along the streamline as in one-dimensional slab flow, it is also possible to calculate from the known earlier-time flow field both the particle velocity and the sound speed at that point from which a sound signal would have had to depart at the earlier time in order to reach the boundary point at the later time. Thus a Riemann invariant can be defined on the streamline, and its value at the

boundary point at the later time can be calculated directly from the particle velocity and sound speed (just found from the known earlier-time flow field), and the assumption of isentropic flow. Then, taking the sound speed at the boundary at its prescribed constant free stream value, the particle speed can readily be computed at the boundary point at the later time. The direction of flow is assumed to be that of the streamline. Hence, the particle velocity can be found as a complete vector quantity. Mass and internal energy are then transported across the downstream boundary at the densities characteristic of the interior of each zone adjacent to the boundary.

Among the gross assumptions involved in this calculation is that of local one-dimensional slab flow. One important source of error in this assumption is its neglect of the contribution to the velocity divergence arising from the spreading of the streamlines. This error can be corrected with little difficulty. A more fundamental objection to the calculation is that, strictly speaking, simultaneously to impose our downstream and upstream boundary conditions is at best redundant, and is otherwise inconsistent with the equations of motion. In supersonic flow, the flow variables have values at the downstream boundary which are not independent of those prescribed at the upstream boundary. Rather, given the initial conditions of the flow, the flow variables downstream are determined by our upstream boundary

values and the equations of motion. All the information needed to update the variables of the motion on the downstream boundary is transmitted on sound signals and particle paths from upstream, and eventually from the upstream boundary alone. (The shock which appears in the supersonic case could be taken into account by a generalization of the artificial viscosity method of Richtmyer and von Neumann.[8,13]) Similar statements hold (but with no shock) for the subsonic case of interest in this program, except that one or more of the upstream boundary conditions could, in principle, be left unspecified while equivalent conditions are prescribed at the downstream boundary; subsonic flow differs from supersonic flow in that news of conditions at the downstream boundary can propagate on sound signals to the upstream boundary. In our latest treatment of the downstream boundary (described above) a rough calculation is made of one piece of data carried by sound signals from upstream; although it has been defined artificially for two-dimensional transient flows, the "Riemann invariant" plays this role in our boundary calculation. The additional specification of the sound speed and the assumption of local isentropic flow overdetermine the motion. The isentropic condition is a convenience which could be done without, in which case the sound speed prescribed at the downstream boundary would still be inconsistent

with the equations of motion unless it were given precisely the values occurring in the flow. Of course, if this information were available, the problem would quite likely already have been solved. If the signals running from boundary to boundary were properly taken into account, it would be unnecessary to prescribe the sound speed at the downstream boundary. On the other hand, to follow these signals would be extremely difficult in a time-marching scheme of solution of the equations of motion. Thus, for practical reasons, we have chosen to employ boundary conditions which are improper in principle.

The justification for our present boundary calculation lies in the fact that the free stream sound speed is often a good approximation to the sound speed along the downstream boundary. For Mach numbers much less than unity, the sound speed varies very little with position in comparison with the other variables of the motion such as velocity. Just as in the case of our first crude boundary calculation, the assumption that the sound speed takes its free stream value at the downstream boundary is accurate sufficiently far downstream. (The calculation is not exact in this limit unless the Mach number is infinitesimal, owing to viscous heating of the gas particles in the wake of the cylinder, and the assumption of adiabatic changes of state.) In the present case, however, "sufficiently far" is almost certainly closer to the obstacle than for the boundary conditions

first used. The philosophy underlying the present boundary calculation is simply that, subject to the requirements that the calculation be stable, and that it lead to accurate results if applied "sufficiently far downstream", "sufficiently far downstream" should be as far upstream as possible in order to save computing time. In our present calculation the troublesome case is that of subsonic flow; for supersonic flow the spurious signals created by a poor downstream boundary calculation never propagate back into the flow field, while on the upstream side the variables can rigorously be given their free stream values.

The imposition of the free stream values of the flow variables along an upstream boundary at a finite distance from the cylinder defines an unconventional, somewhat artificial, but quite possible, subsonic flow problem. Of course, the farther this boundary is placed upstream, the more closely the problem so posed will coincide with the usual one in which the free stream boundary conditions are specified at infinity. Again, just as for the downstream boundary, the upstream boundary has been placed close to the cylinder in order to conserve computing time, but (hopefully) not so close as to create a much different flow than if the boundary were far upstream.

The assumptions of the present treatment of boundaries become more and more exact as the Mach number is reduced to zero,

and are entirely consistent with the equations of motion for Mach numbers greater than one. A test of this boundary calculation was therefore felt to be desirable.

Velocity fields computed with the two boundary conditions are shown in Figures 16 and 17. The medium mesh and a Reynolds number of 1000 were used in these calculations. The velocity field of Figure 16 represents a later stage of the flow of Figure 15, which in turn developed from impulsive initial conditions. The flow field corresponding to Figure 17 was also calculated from that represented by Figure 15; in this case the Figure 15 flow field was used as initial-time data and the problem was continued with the new downstream boundary equations. The velocity field of Figure 16, which exhibits zone-by-zone oscillations in both direction and amplitude, has been appreciably smoothed in Figure 17, although zone-by-zone amplitude fluctuations are seen; it is felt that these fluctuations reflect the velocity variations of the "initial-time" data corresponding to Figure 15, although this point has not been checked. At present, the most convincing evidence of the soundness of the new boundary calculation is contained in Figures 18 - 37. While the diffusion of vortices with the new boundary equations is still seen to be serious near the downstream boundary, the diffuse region shows no tendency to propagate upstream; evidently neither the vortex shedding

process nor the vortex street have been interfered with after thousands of time-steps, during which many sound signals have traversed the region between the boundaries. Such diffusion as may be observed is probably due more to the coarseness of the mesh near the downstream boundary than to errors inherent in the boundary calculation.

3.4 Vortex Street Formation

The downstream boundary condition just discussed was used only in the problem which has a Reynolds number of 100. This problem was begun with the values of the flow field variables found for a Reynolds number of 10,000 after 600 time-steps of computation. At this point, the Reynolds number was changed to 100 and the calculation was continued with no other changes for 1290 more time steps. Instead of being perfectly circular, the cylinder cross section in this problem was a circle slightly flattened in the neighborhood of a point opposite one of the lateral boundaries of the problem; i.e., the cylinder cross section was circular except for a small segment consisting of a straight line parallel to the free stream flow direction. This deformation was accomplished simply by setting the x-coordinate of one of the two cylinder boundary points on the line $y = o$ equal to the x-coordinate of the two adjacent points on the cylinder boundary. The system was thereby deliberately rendered unsymmetrical to a slight degree - but much more than would be the result of the careful machining of a cylinder a few centimeters in diameter. The purpose of introducing asymmetry into the problem was to bring about the shedding of vortices with the consequent growth of a vortex street, in keeping with the results of experimental observation. After 1290 cycles, the velocity field

plots showed vortices on either side of the y-axis which were perceptibly different from mutual mirror images. However, their asymmetry fell far short of that associated with imminent vortex shedding, even though 1290 time-steps is longer than the observed time between the shedding of two vortices for this Reynolds number [14] and long enough for a sound signal to move three times the distance between the upstream and downstream boundaries. It was therefore decided to go back 390 time-steps and introduce a much stronger symmetry perturbation into the problem by setting the particle velocity equal to zero at each of a group of mesh points near the flattened portion of the cylinder on its downstream side, before running the problem further. The velocities at these points were computed thereafter according to the equations of motion; they were not forced to remain zero. This asymmetric disturbance of the flow field proved sufficient to initiate the shedding of vortices, the first of which detached itself from the side of the cylinder opposite to that on which the perturbation was introduced. Figures 18 - 37 show the velocity field in increasing time sequence, from its impulsive start with a Reynolds number of 10,000, to the almost streamlined velocity field which soon develops from the initial field as the flow adjusts itself to the presence of the cylinder, to earlier and later stages of the almost symmetrical growth of the first vortices formed behind the cylinder after the Reynolds number was changed to 100, through the shedding of several vortices at various times after the small group of

particle velocities was set to zero in order to create a major asymmetry in the flow field. In all, the calculation was carried through the shedding of five vortices; 4900 time-steps were taken in the course of the calculation at a rate of about 25 minutes per hundred time-steps on the CDC 3600 (and slightly longer on an IBM 7094 II).

After many vortices have been shed, the experimentally observed result of the shedding process is a periodic flow field in which a vortex detaches itself first from one side of the cylinder, then from the other side, and so on. The computer code output was examined closely in the interval following the formation of the next-to-last vortex shed; in this way an estimate of the period of the flow was obtained, which was as free as possible of the transients introduced by the initial conditions of the problem. The velocity field plots were inspected to determine when the center of each of the last two vortices shed coincided with a particular value of the y-coordinate. This was done for two different values of y, namely, $y = 4.0$ and $y = 7.0$. By doubling the difference between the arrival times of successive vortices at a given value of y, an approximation to the flow period was obtained from the numerical results. Making use of the numerical values assigned to the relevant parameters of the system, this period was converted to a dimensionless flow field

frequency known as the Strouhal number.‡ The two values obtained in this way from the data taken at the two y-positions are 0.16 and 0.18. For a Reynolds number of 100 the experimental value of the Strouhal number is 0.17. This is perhaps the most significant quantitative check which we have made of the validity of the numerical data generated in the program. The fact that the periods estimated at y = 4.0 and y = 7.0 are not the same may be due to errors in determining from the velocity plots (which were made at intervals of 100 time-steps) just when the eye of a vortex lies on a given line of constant y; or it may be evidence of numerical solution errors, particularly those stemming from the boundaries; or the flow may actually not yet have become periodic. In any case the two periods are not much different.

Another, and cruder, check on our results lies in the fact that the calculations for a Reynolds number of 5000 predict a flow field free of vortices (see Figure 38). It cannot be claimed that a turbulent wake has been calculated in this case, but the code has clearly predicted that vortices will form at a Reynolds number of 1000, and not at 5000. Experimentally, it has been found that a transition from vortex streets to turbulent wakes takes place in this range of Reynolds numbers.[7]

‡ The Strouhal number[15] is defined as S = nD/v; where n is the shedding frequency; v the free stream velocity; and D a characteristic dimension of the body, e.g., the diameter of the cylinder.

3.5 Pressures, Pressure Fluctuations, and the Transition to Turbulence

Experimental measurements of the pressure at various points on the cross-section of a right circular cylinder are available at several instants of time in the early stages of impulsively initiated motion.[16] These pressure values are compared in Figure 39 with the results of our medium mesh calculations for a Reynolds number of 1000. The shapes of the experimental and theoretical curves are generally similar. The extent of agreement between the two suggests that useful estimates of the stress on an obstacle in the flow field can be obtained for flows of this kind without further refining the mesh. However, when the fine mesh was used, it was found that the computed and experimental results did not agree as well as with the medium mesh (see Figure 40). Zone-by-zone pressure oscillations appear which are of appreciable amplitude, so that even though the mean pressure over a few zones has a value close to that given by experiment, the detailed picture is not adequate for quantitative purposes. Of particular concern is the fact that signals of high frequency (either in space or time) predicted by finite difference calculations, are often quirks of the numerical method with no physical significance. It was therefore natural to ask whether corresponding fluctuations took place time-step by time-step, or at most over the course of a few time-steps. Accordingly, the computed values

of the pressure were plotted as a function of the time-step for each of four contiguous zones adjacent to the cylinder at the downstream-most part of its surface. The results shown in Figure 41 indicate a smooth variation of the pressure with time which, while not periodic, is nearly so for each zone. All the curves are similar in this respect, but are clearly out of phase (as noted in Section 1.0), and the result at an instant of time approaches spatial randomness. A mean period of about one hundred time-steps can be assigned to these curves, which is much longer than the time required for a sound signal to traverse the zones in this region of the flow, and is also much longer than the time required for a particle in the free stream to move a distance comparable to the zone width. Since the pressure oscillations have a mean period of many time-steps, and this period has no apparent correlation with signal or particle transit times across zones of the finite difference mesh, the conclusion reached tentatively here is that these fluctuations are physical, and not mathematical, in origin. It has been postulated[17] that vortices include small-scale turbulent motion whose amplitude increases with Reynolds number to the point where the turbulence is so severe that smooth flow cannot take place on a scale large enough for vortex formation. It is possible that the pressure fluctuations observed here are evidence of such turbulent motion.

4.0 RECOMMENDATIONS AND CONCLUSIONS

4.1 Right Circular Cylinders, Perfect and Perturbed

In this program a first attempt has been made to apply our specific finite difference techniques and the computer codes based on them to the flow of a compressible viscous fluid around an obstacle. While the results obtained have been encouraging, they represent little more than a start on the use of these numerical methods to help explain the mechanisms involved in vortex and turbulent wake formation; with regard to the exploitation of the technique in all its fields of application, or even in aerodynamic applications alone, the problems solved here are a minute beginning. More extensive investigations need to be made of the mathematical aspects of the method, i.e., the role of its mathematical parameters, as well as of the effects of the variation of physical parameters in specific practical applications. In addition, even the small amount of work reported here has pointed out a need for new experimental work. The number of experiments suggested by the results of numerical computations like these is almost certain to grow rapidly as the range of application of the technique is widened.

A more complete check of the flow fields predicted by the computer code is presently the most important task to be performed in connection with our flow field calculations. Many more such

checks can be made even for the circular cylinder problems studied here. Code runs like that described in Section 3.0 for a Reynolds number of 100 should be made for other Reynolds numbers, and a curve of Strouhal number vs. Reynolds number should be prepared from the results of these calculations for comparison with the experimental curve already available.[14] The expense involved in generating the individual points of this curve might be considerably reduced over that incurred in this program for the single point at a Reynolds number of 100, by incrementing the Reynolds number in small steps. If the output generated for one Reynolds number is used as initial time data for a slightly different Reynolds number, then the flow field may adjust itself relatively quickly to the new Reynolds number, and it may only be necessary to compute the flow through the shedding of two or three vortices.

Another form of experimental data available for quantitative comparison with code output consists of photographs of flow fields showing streaks created by the extrusion of dye into the fluid from various points on the cylinder.[18] To produce corresponding output from the computer codes would require the programming of a special service routine for processing the primary code output; no modification of the code itself would be necessary. Along these lines, our plot routine could be changed slightly to generate the instantaneous streamlines of a flow field.

A further kind of quantitative check between the computed and experimental data lies in a comparison of pressures at various points in the flow field. Great care needs to be exercised in making this comparison owing to the high-frequency pressure fluctuations predicted by the computer code. A space-time average of the pressure, corresponding to the detailed experimental conditions, would probably be the proper quantity to compare with experimental data.

A number of other problems of viscous compressible flow around a right circular cylinder, whose solution would be of widespread interest, come to mind. For example, the computer code could be used to predict more closely a critical Reynolds number associated with the transition from vortex formation to turbulence. In the same vein, calculations like those reported here could be carried out to account for the critical Reynolds number ($R \approx 40$) associated with the transition between vortex street flows and flows characterized by standing vortices. Such a study would involve the variation of the Reynolds number over a very small range relative to that used in this program. The code output provides detail which could be of help in understanding the processes involved in these transitions. It might also be possible to determine whether truly "critical" Reynolds numbers reall

exist, and how blurred these might become under the influence of various disturbances. Such data could be useful in designing experiments for the study of transitional flow phenomena. More generally, the influence of perturbations of different kinds on the outcome of flow field experiments could be helpful in explaining discrepancies in observed experimental data.

With regard to perturbations, an experiment is suggested by a result noted earlier (Section 3.0), namely, that the symmetry of the flow field must be grossly perturbed in order to induce vortex shedding; a slight - but definitely macroscopic - flattening of one side of the cylinder resulted in a very slow growth of asymmetry. Thus, taking pains to insure the symmetry of initial and boundary conditions, it might be possible to design an experiment whose outcome would be the growth of vortices in which circulation is accumulated without shedding for a time interval much longer than the normal shedding period. This kind of vortex growth should probably be confirmed first by more detailed calculations. If experimental data then agree with the computed results, basic information will have been obtained on the stability of vortex flows. If not, it would be natural to ask by what mechanism symmetry is destroyed; the answer would then appear to be basic to an understanding of vortex growth and shedding under transient (i.e., non-periodic) conditions.

Next, other flow parameters than the Reynolds number could be varied, and particularly the Mach number. A study of the effect of this parameter over a range which includes exactly sonic upstream boundary values could be made with no significant changes in the present computer program. For such a study it might be desirable to consider more realistic behavior of the pressure than that of a polytropic gas. Since the calculation of the stress takes place in one subroutine of the computer program, a more complicated equation of state for air (or an entire constitutive equation) could be introduced into the calculations by reprogramming this single subroutine.

An increased understanding of the mechanisms controlling the main features of the flows calculated in the program might be obtained by examining more carefully than has been possible up to now the numerical results already at hand. Each code calculation can be looked upon as a computer experiment, and in fact is in some ways more closely related to a physical experiment than to a conventional theoretical calculation of flow phenomena. Actually, the code runs have the advantage of offering much more detailed flow field information than do actual physical experiments. A careful, thorough study of the voluminous output generated in this program might, for example, lead to the "empirical" discovery of a relation between the vortex shedding frequency and other parameters of the system.

4.2 Pressure Fluctuations; Everywhere Discontinuous Flow Fields

With respect to increased physical insight, perhaps the most interesting new application of the finite difference technique lies in the study of the pressure fluctuations described in Sections 1.0 and 4.0. It appears highly desirable to find out whether or not these fluctuations are physically real. This could be done by repeating the calculations with more and more refined finite difference meshes. Several separate code runs should be made, up to the limit of reasonable cost on existing computers. The most advanced computers now available make practical the use of at least eight times as many mesh points as there were in the medium mesh of this program. Plots of pressure vs. time similar to Figure 40 could then be made, and the characteristics of these curves - particularly the amplitude of the pressure fluctuations - studied as a function of the mesh point density. If the pressure fluctuation amplitude shows no systematic tendency to decrease as the mesh point density is increased, then the physical reality of these fluctuations will have been established, to the extent that it is possible to do so by our finite difference methods. At this point it would be necessary to appeal to experiment either to verify or deny the code predictions. Hot wire probes might be used in these experiments, but the experimental apparatus would have to be

designed to operate at frequencies of at least 50 kilocycles, which is considerably higher than usual.

The study of pressure fluctuations has another aspect of great potential significance to the theoretical treatment of viscous flow. It has been noted that these fluctuations vary smoothly with time, but (within the limits of resolution of our finite difference mesh) they appear to vary very rapidly with spatial position. The implications of similar behavior for finer and finer finite difference meshes would be weighty. In that case, the numerical technique would have predicted a pressure field varying continuously in time, but with no spatial continuity at all. The possibility of everywhere discontinuous solutions of the flow equations, or of solutions with everywhere discontinuous low-order derivatives, has been mentioned before.[19] If these are indeed the kinds of flow fields implied by the underlying principles of motion for viscous compressible media, then the representation of these principles as differential equations is not valid for these flows. More general integral statements of the governing principles of continuum mechanics would have to be used as their mathematical form.[2] Finite difference techniques which, like those employed here, make no continuity assumptions for the flow variables other than Riemann integrability, and which are direct finite difference expressions of the laws of motion in

integral form, could reasonably be expected to predict correctly such flow fields. It is difficult even in principle to see how these fields could be calculated by classical analytical techniques based on the differential equations of motion (as they almost always are), if the spatial derivatives appearing in these equations do not exist. Finite difference methods based on the "differencing" of the differential equations of motion may be similarly limited. Thus, the further study of the pressure fluctuations noted here would appear to be very worthwhile from both the physical and mathematical points of view.

4.3 Airfoils; More General Plane-Symmetric Systems and Boundary Conditions

The variety of systems which can be treated by the methods employed in this program is very wide; only a few such systems will be cited now. First, it would be straightforward to calculate specific flow fields for right cylinders which are not of circular cross section. In fact, to the extent that airfoil flows can be described as two-dimensional plane-symmetric problems, the automation of airfoil design is a distinct possibility. To determine the density and distribution of mesh points required for this purpose, calculations of lift and drag could be made for several of the large number of airfoils for which lift and drag have been measured experimentally. A comparison of the computed and observed results would also serve as a further check on the general validity of the numerical method. The automation of airfoil design could then be brought about by using the entire present computer program as a subroutine in a larger program which systematically varies any desired design parameters and optimizes the airfoil with respect to some predetermined criterion. The optimization procedure could be given almost any useful degree of complexity, in view of the amount of computation required to predict a single flow field. Again, to reduce the length of time required for each flow calculation, advantage might be taken of

the fact that the successive flows of an optimization process would differ by small variations in the design parameters.

The calculations made here could be extended to systems containing more than one cylinder, circular or otherwise, and ultimately to periodic arrays of cylinders. Subject to the limitations of computing cost, mutual interaction effects in such systems could be predicted numerically. It is perhaps more practical at the present time to apply the computer code to the flow of a viscous compressible medium around a rotating cylinder, or a cylinder undergoing periodic radial oscillations. More generally, the code could be modified to include almost any prescribed motion of the cylindrical surface and almost any frictional condition at that surface from a no-slip law to free sliding. In this connection, time-varying boundary conditions could be imposed at any boundary in the system. Thus, for example, flow fields might be calculated in the neighborhood of a cylinder exposed to gusts or periodic blasts of air. Another kind of physical effect which could be taken into account is that of a difference in temperature between the cylinder and the fluid in contact with it. The finite difference equations and the computer code would have to be modified in this case to include the transport of energy by thermal conduction.

4.4 Scope of the Numerical Method; Other Geometrics, Constitutive Equations and Coordinate Systems

The method used to develop the finite difference equations on which the calculations of this program were based applies in principle to the entire range of continuum mechanical phenomena.[1-4] The computer codes embodying the difference equations were written with the explicit intention of achieving this generality in practice. Finite difference equations have been developed not only for the two-dimensional plane-symmetric case, but for the linear, cylindrical and spherical one-dimensional motions of an isotropic medium, for two-dimensional motion with axial symmetry, and for general transient motion in three space dimensions. The difference equations involved form a hierarchy in which, within the limits of geometric possibility, the equations of higher spatial dimensionality reduce to those of lower dimensionality when appropriate symmetry assumptions are made. Moreover, they take into account general stresses and strains. Corresponding computer codes have now been written for the three cases of one-dimensional motion, as well as for plane symmetric two-dimensional motion. A computer program is currently under development for the treatment of axially symmetric two-dimensional systems, as the second phase of an Air Force program whose goal is the theoretical prediction of the ground

motion resulting from a nuclear explosion. In fact, the plane two-dimensional computer code used here was developed in the first phase of the Air Force program as an aid in the study of our method of constructing finite difference equations, prior to work on the axially symmetric case. The code for axisymmetric motion is expected to be completed soon. It will be used (among other things) for further calculations of viscous compressible fluid flow, as part of an extension of the program described in this report. An obvious application for this computer code is to the motion of a variety of axially symmetric objects in the atmosphere. It is expected that the code will be capable of predicting the drag on cones and other axisymmetric bodies as a function of Reynolds number, Mach number, and the shape parameters of the body. It is worth noting that in either the plane or axisymmetric cases, the finite difference equations are sufficiently general to permit a description of the obstacle as an object with a constitutive equation of its own, and to allow the obstacle to deform under the action of the surrounding medium. If the obstacle has a much higher sound speed than the medium around it, a difficult practical problem might arise in that, for reasons of numerical stability, the flow calculation would require an enormous number of time-steps to cover a time interval significant

to the development of the flow field around the obstacle. In such cases it might be practical to treat the body first as rigid, making a flow field calculation like those of this program. The forces on the rigid obstacle could then be imposed as boundary conditions which give rise to motion in the obstacle. Next, the resulting obstacle boundary motion might be used as a boundary condition for another calculation of the surrounding flow field, thus generating new forces on the surface of the obstacle, etc.

It is worth commenting on one further aspect of the generality of the finite difference equation used here, namely, that these equations have been written in an arbitrary time dependent coordinate system. Thus, the possibility of using a spatial mesh which deforms in some prescribed manner as a flow progresses, was deliberately taken into account in the original formulation of the equations of motion. In the work of this program, it was natural to use an Eulerian coordinate system; the generality of the equations with respect to coordinate systems was helpful in this program only in that it readily permitted the use of an Eulerian coordinate system which was not Cartesian. For supersonic flows, and perhaps others, it might be desirable to have special surfaces in the flow field, such as shock fronts, as coordinate surfaces. More generally, it is reasonable to expect greater accuracy in the solution obtained with a given

number of mesh points if the density of points is allowed to adjust itself to the instantaneous conditions of a flow; then the mesh point density will automatically become greatest where the need for spatial definition is greatest. Considerable progress has already been made in the definition of such coordinate systems. Its most important application in aerodynamics is probably to atmospheric motion, where phenomena of great importance can occur on vastly different scales of distance and time.

It has been a hopeful sign of the validity of our approach to the construction of finite difference equations, that a computer code intended to describe the motion of earth materials can yield quantitatively useful results for viscous compressible fluid flows. The general continuum motion equations are independent of the properties of the media to which they may be applied in specific cases. It is our feeling that this should also be true of any finite difference equations for continuum motion, not only in the obvious sense that the calculation of stress should be cleanly separated from the calculation of the other variables of the motion, but also in the sense that the finite difference equations should work about as well for one material as for another. The finite difference equations used here have met this test well for Stokesian fluids and for solids. The extent to which this state of affairs will obtain for other materials of physical interest remains to be seen.

REFERENCES

1. Trulio, J. and Trigger, K., "Numerical Solution of the One-Dimensional Hydrodynamic Equations," UCRL 6267 (1961).

2. Trulio, J. and Trigger, K., "Numerical Solution of the One-Dimensional Hydrodynamic Equations in an Arbitrary Time Dependent Coordinate System," UCRL 6522 (1961).

3. Trulio, J., Chapter 3, Vol. III, Methods in Computational Physics (Academic Press, 1964).

4. Trulio, J., "Studies of Finite Difference Equations for Continuum Mechanics," WL-TDR-64-72 (1964).

5. Fromm, J. and Harlow, F., Phys. Fluids, 6, 975 (1963).

6. Fromm, J., Chapter 10, Vol. III, Methods in Computational Physics (Academic Press, 1964).

7. Schlichting, H., Boundary Layer Theory, p. 30, 4th Ed., (McGraw-Hill, 1960).

8. Richtmyer, R. and von Neumann, J., J. Appl. Phys., 21, 232 (1950).

9. Hoskin, N.E., Chapter 7; Richardson, D.J., Chapter 8; Methods in Computational Physics (Academic Press, 1964).

10. Courant, R., Friedrichs, K., and Lewy, H., Math. Ann., 100, 32 (1928).

11. Ref. 7, pp 30, 222.

12. Ref. 7, p 28.

13. Schulz, W., Chapter 1, Vol. III, Methods in Computational Physics (Academic Press, 1964).

14. Roshko, A., "On the Development of Turbulent Wakes from Vortex Streets," NACA Rep. 1191 (1954); see also Ref. 7, p 31.

15. See Ref. 7.

REFERENCES

16. Schwabe, M., Uber Druckermittlung in der instationaren ebenen Stromung. Ing.-Arch. 6, 34 (1935); NACA TM 1039 (1943)

17. Ref. 7, p 17.

18. Ref. 7, p 457.

19. To the author's best recollection of a long-past conversation, this suggestion was attributed to Professor G. Birkhoff of Harvard University.

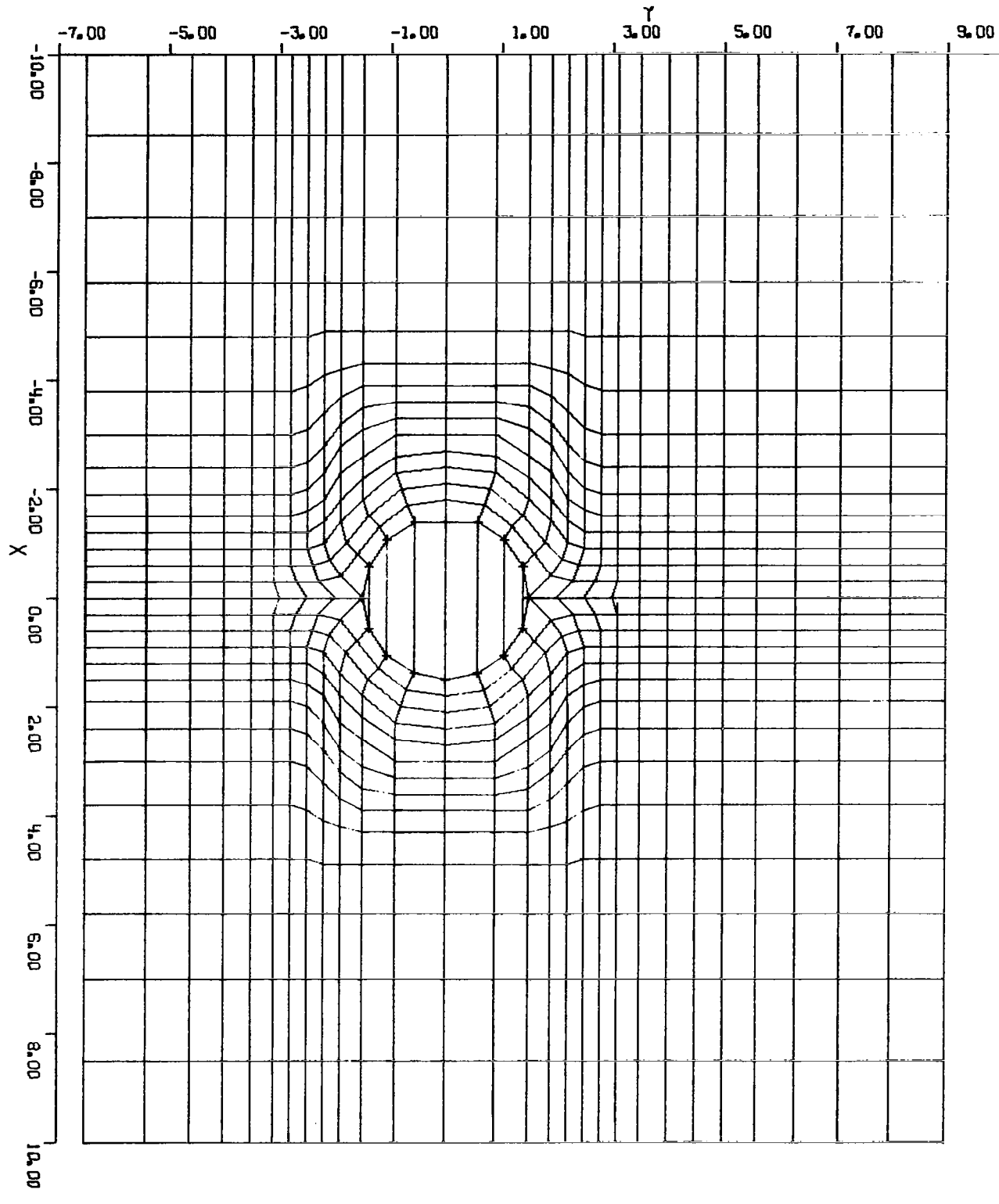

Fig. 1. Coarse Mesh (29 x 29)

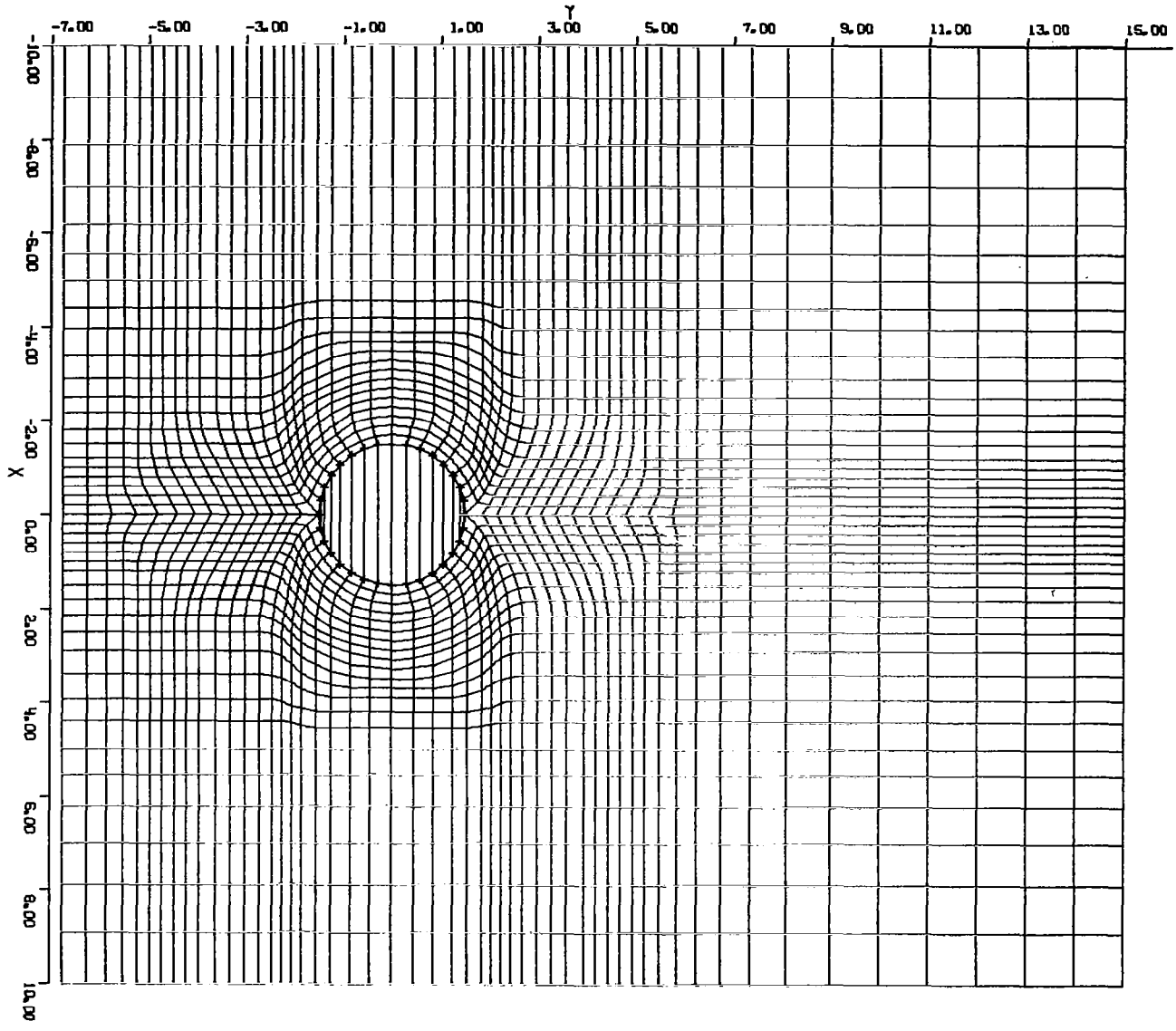

Fig. 2. Medium Mesh (43 x 48)

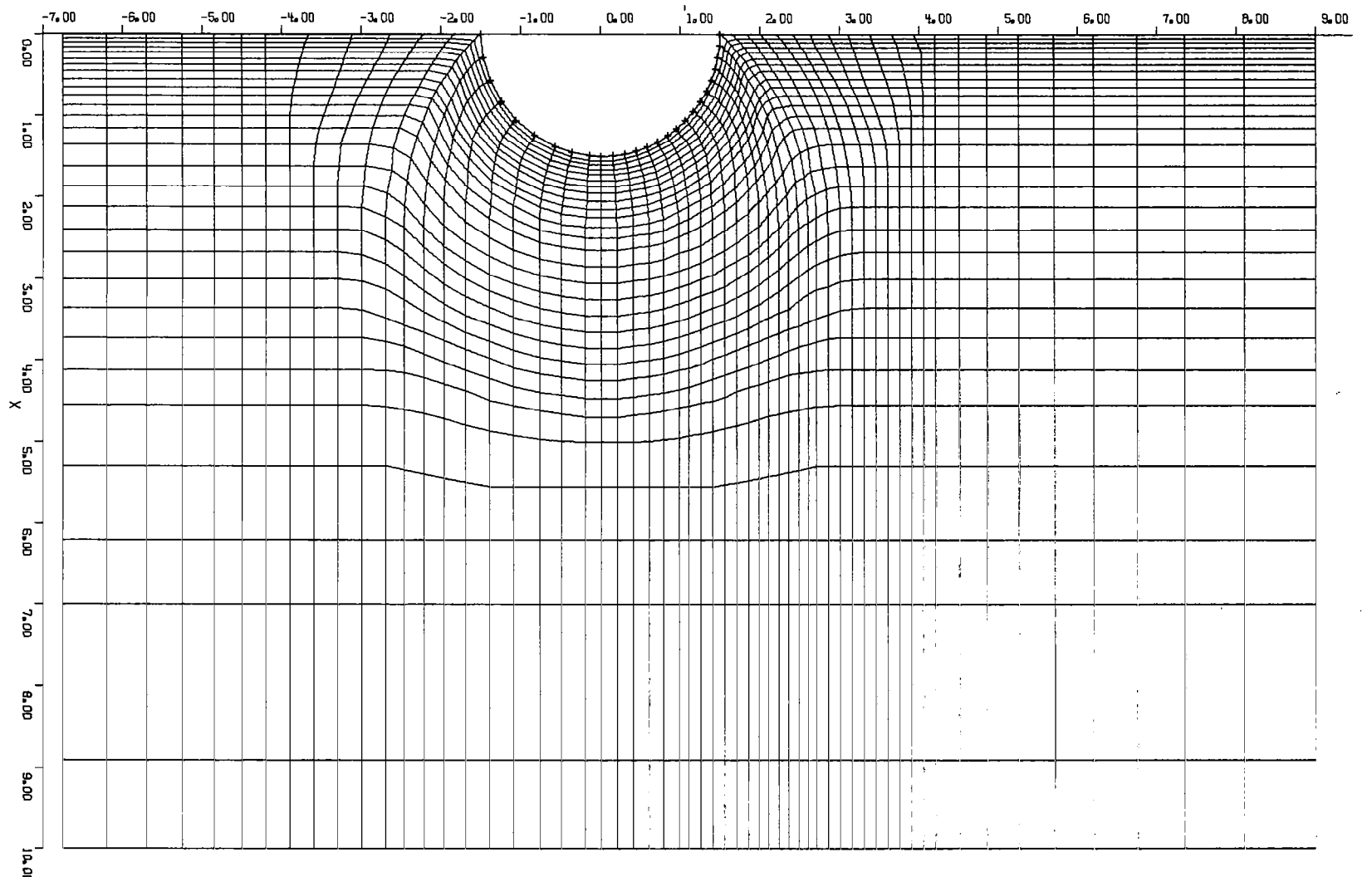

Fig. 3. Fine Mesh (59 x 59).

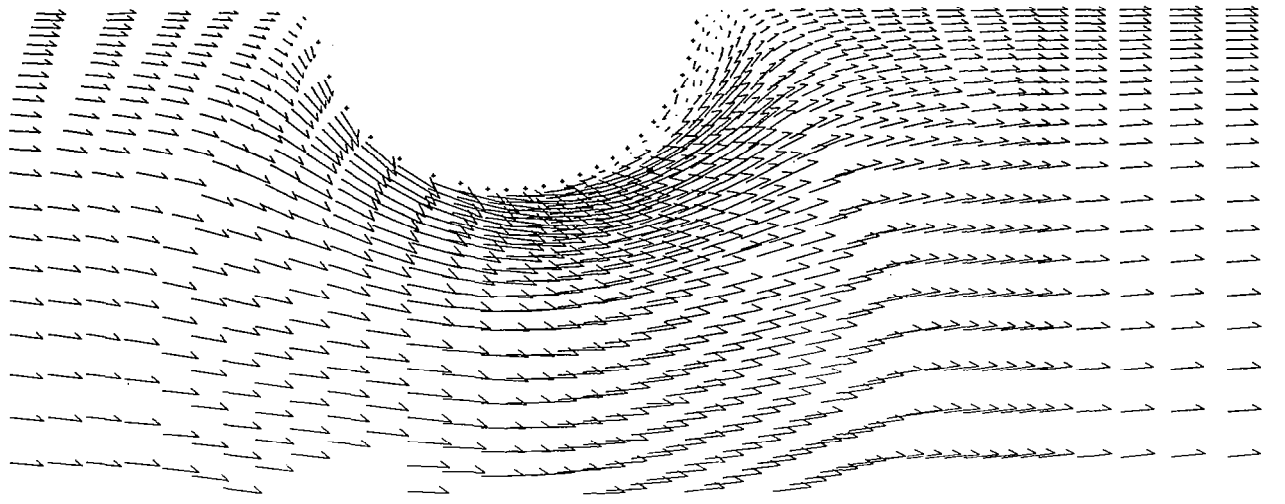

Fig. 4. Problem No. 112.1, R = 1000, Fine Mesh; Free stream particles have moved 0.529 cylinder diameters.

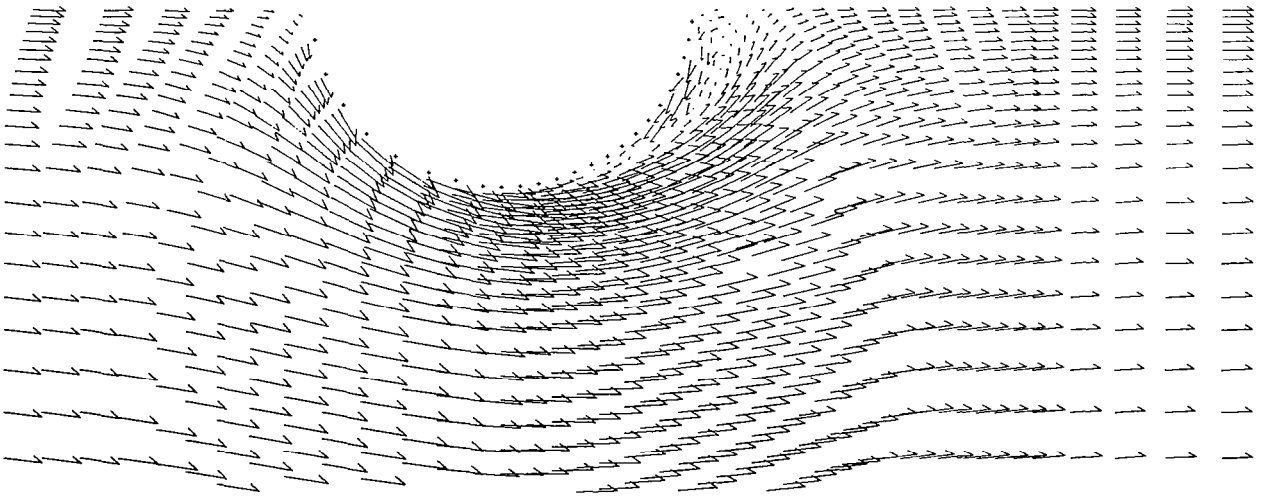

Fig. 5. Problem No. 112.1, R = 1000, Fine Mesh; Free stream particles have moved 0.795 cylinder diameters.

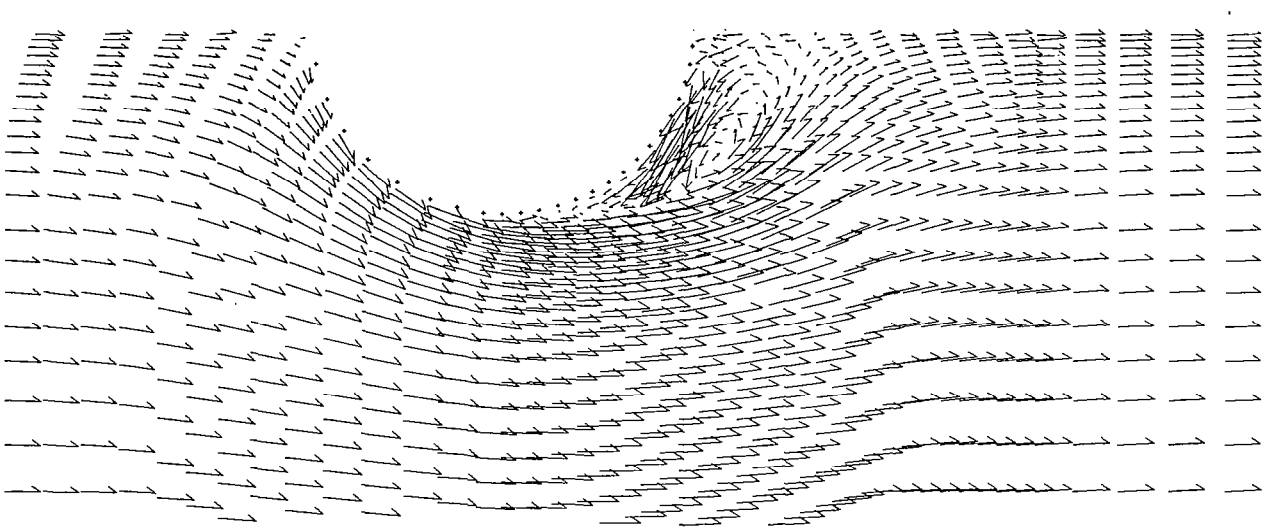

Fig. 6. Problem No. 112.1, R = 1000, Fine Mesh; Free stream particles have moved 1.25 cylinder diameters.

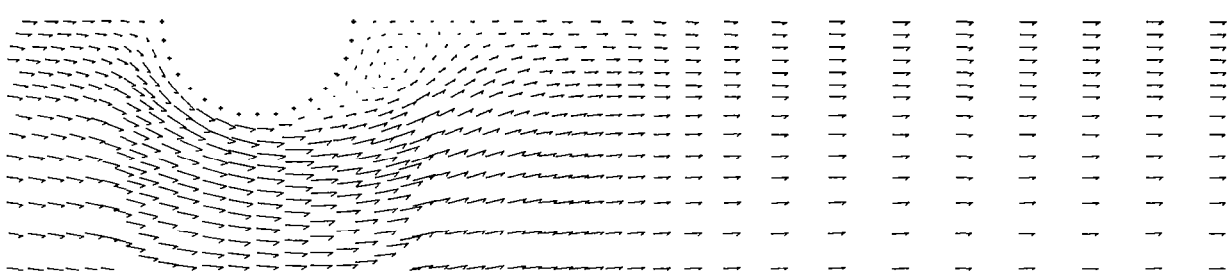

Fig. 7. Problem No. 211.3, R = 1000, Medium Mesh; Free stream particles have moved 1.19 cylinder diameters.

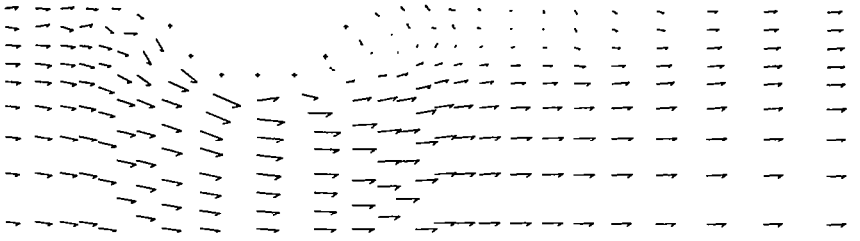

Fig. 8. Problem No. 208.3, R = 1000, Coarse Mesh; Free stream particles have moved 1.19 cylinder diameters.

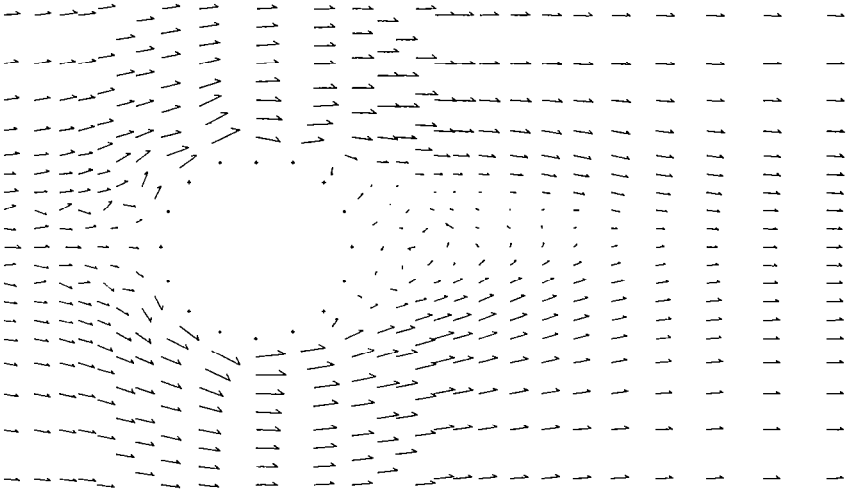

Fig. 9. Problem No. 208.3, R = 100, Coarse Mesh; Free stream particles have moved 0.395 cylinder diameters.

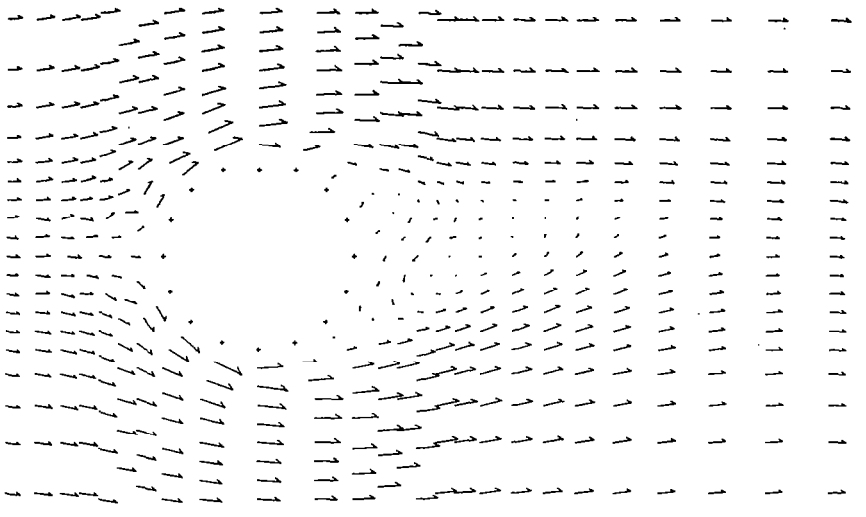

Fig. 10. Problem No. 208.3, R = 100, Coarse Mesh; Free stream particles have moved 1.19 cylinder diameters.

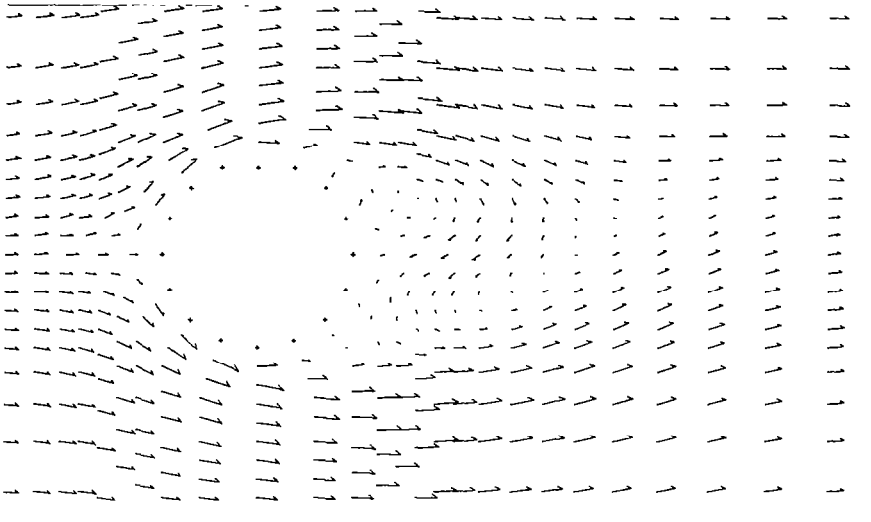

Fig. 11. Problem No. 208.3, R = 100, Coarse Mesh, Free stream particles have moved 2.37 cylinder diameters.

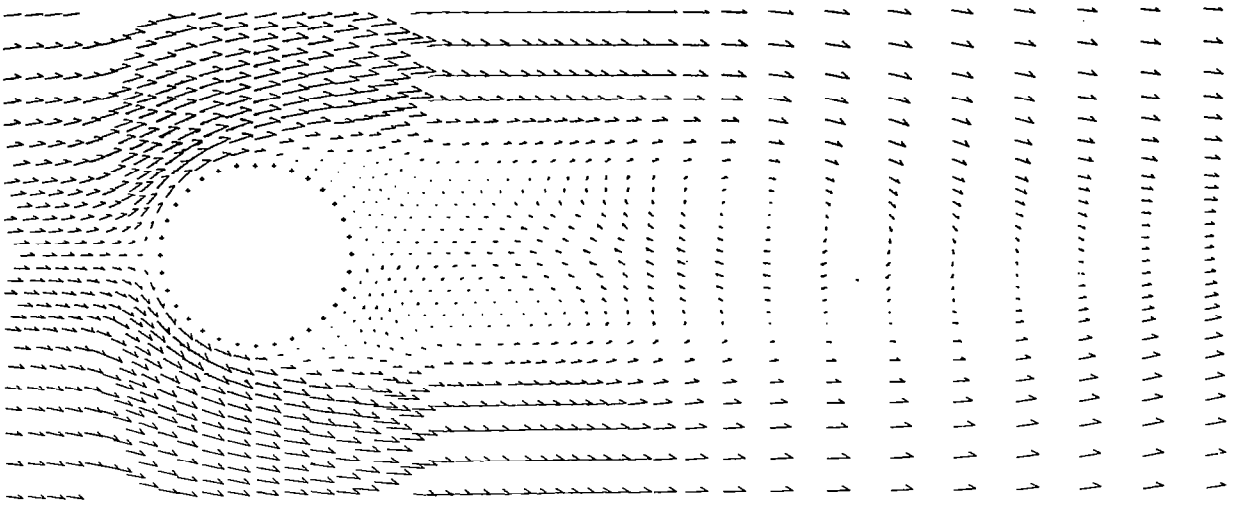

Fig. 12. Problem No. 211.41, R = 100, Medium Mesh; Free stream particles have moved 0.4 cylinder diameters.

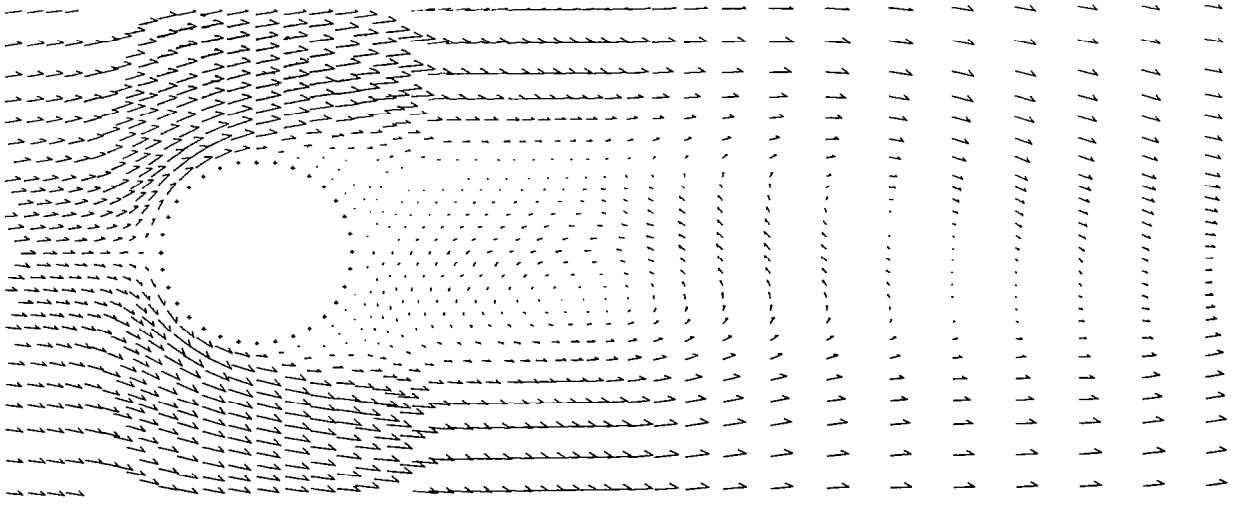

Fig. 13. Problem No. 211.41, R = 100, Medium Mesh, Free stream particles have moved 1.2 cylinder diameters.

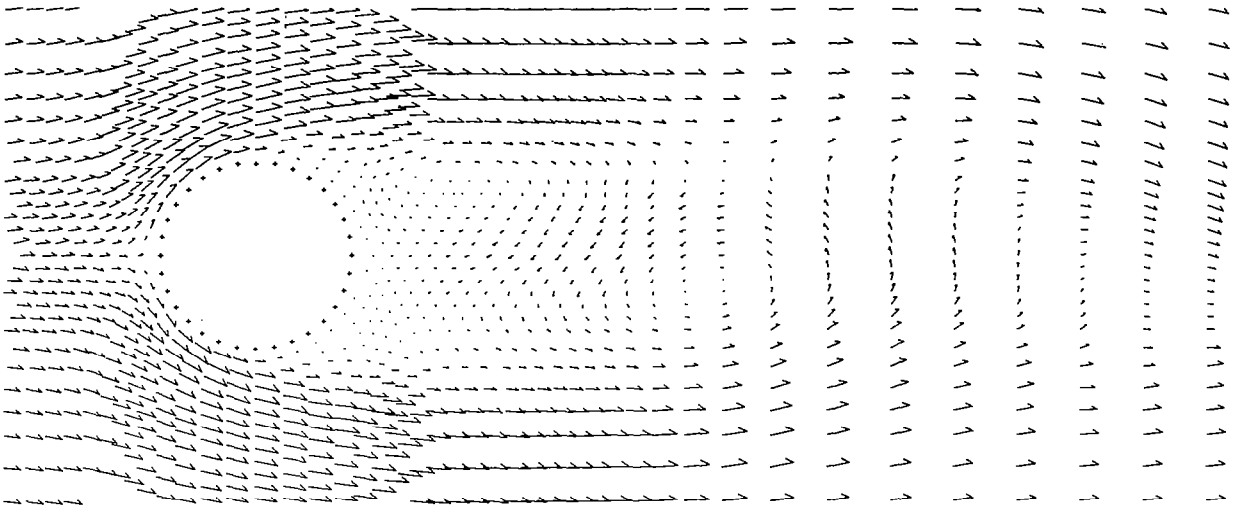

Fig. 14. Problem No. 211.41, R = 100, Medium Mesh; Free stream particles have moved 2.4 cylinder diameters.

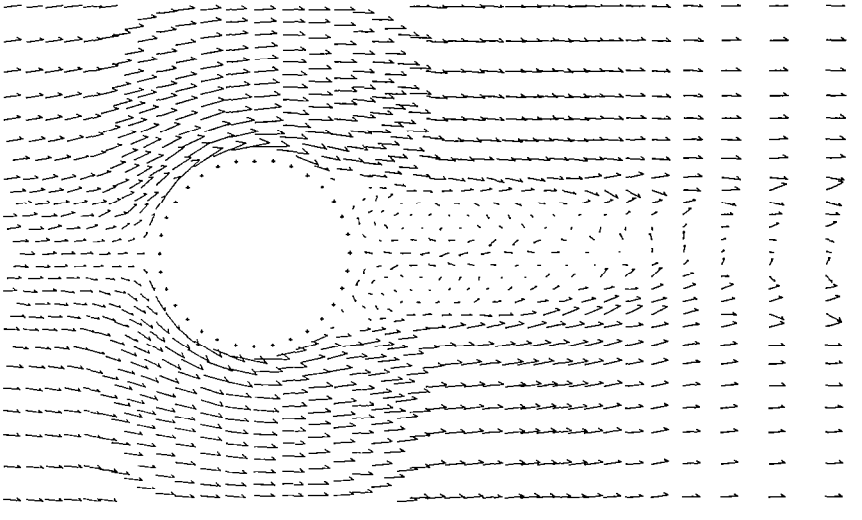

Fig. 15. Problem No. 209, R = 1000, Medium Mesh; Free stream particles have moved 7.17 cylinder diameters; A non-physical signal arising from the crude boundary calculation has moved from the downstream boundary to about 2.11 cylinder diameters from the center of the cylinder.

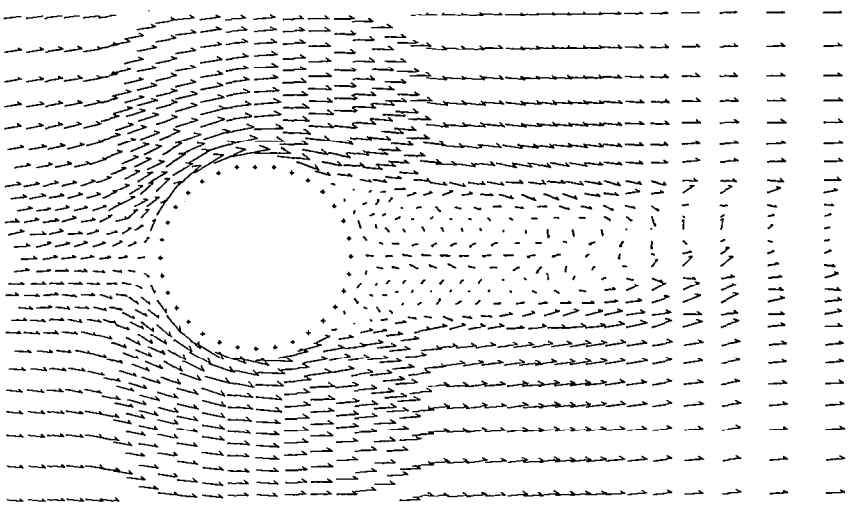

Fig. 16. Problem No. 209, R = 1000, Medium Mesh; Free stream particles have moved 7.95 cylinder diameters; a non-physical signal arising from the crude boundary calculation has moved from the downstream boundary to about 1.9 cylinder diameters from the center of the cylinder.

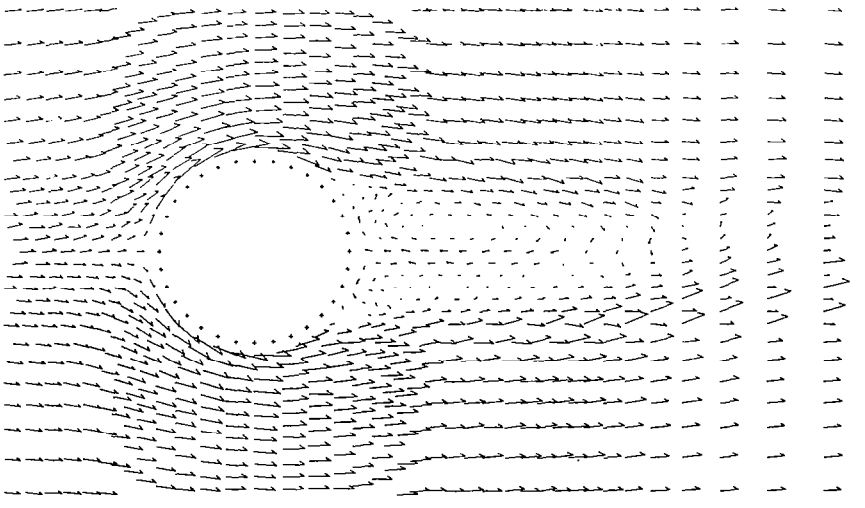

Fig. 17. Problem No. 209, R = 1000, Medium Mesh; Free stream particles have moved 7.95 cylinder diameters. This problem was restarted from the configuration of Figure 15 and run with the new boundary condition.

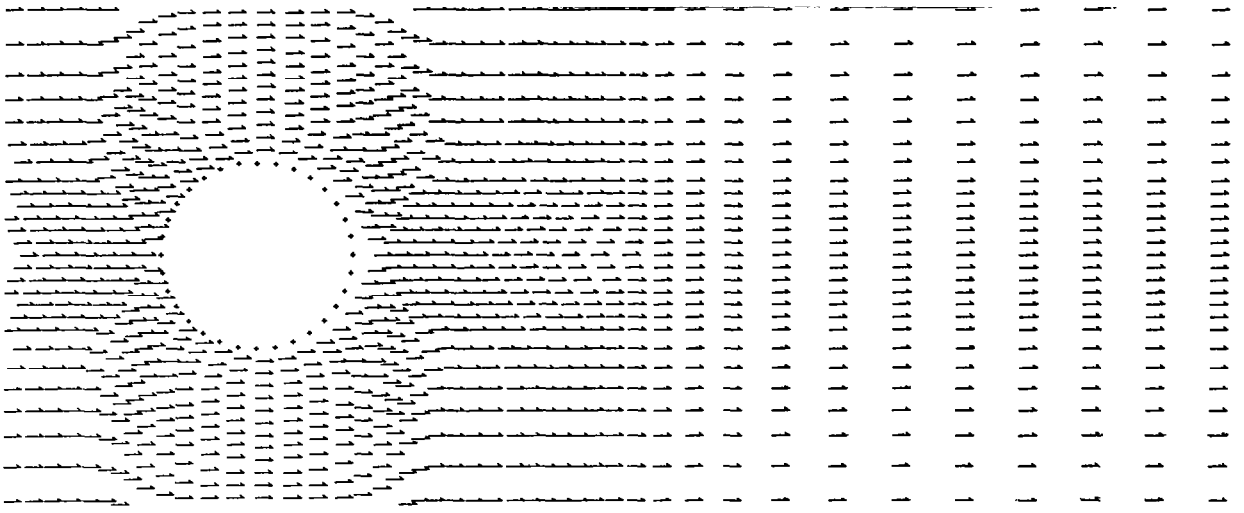

Fig. 18. Problem No. 211.3, R = 100, Medium Mesh; Old boundary condition; Free stream particles have moved 0.0 cylinder diameters.

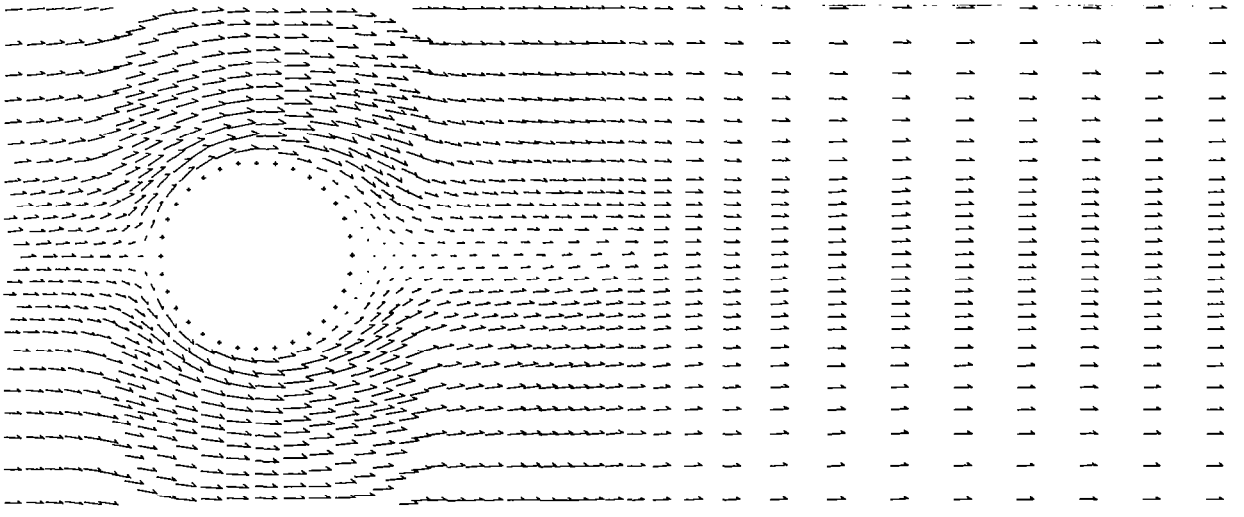

Fig. 19. Problem No. 211.3, R = 100, Medium Mesh; Old boundary condition; Free stream particles have moved 0.397 cylinder diameters.

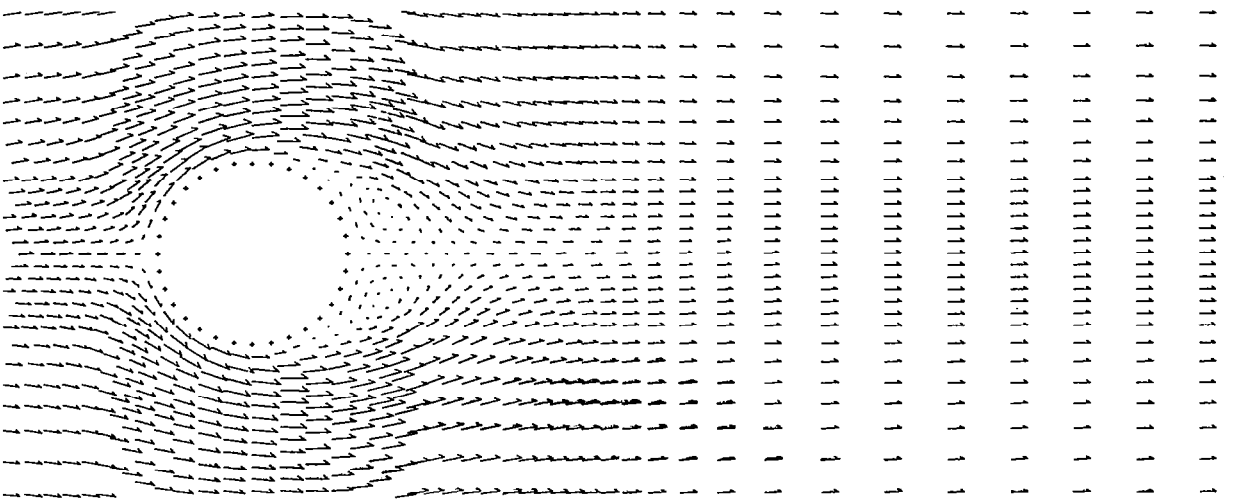

Fig. 20. Problem No. 211.3, R = 100, Medium Mesh; Old boundary condition; Free stream particles have moved 1.19 cylinder diameters.

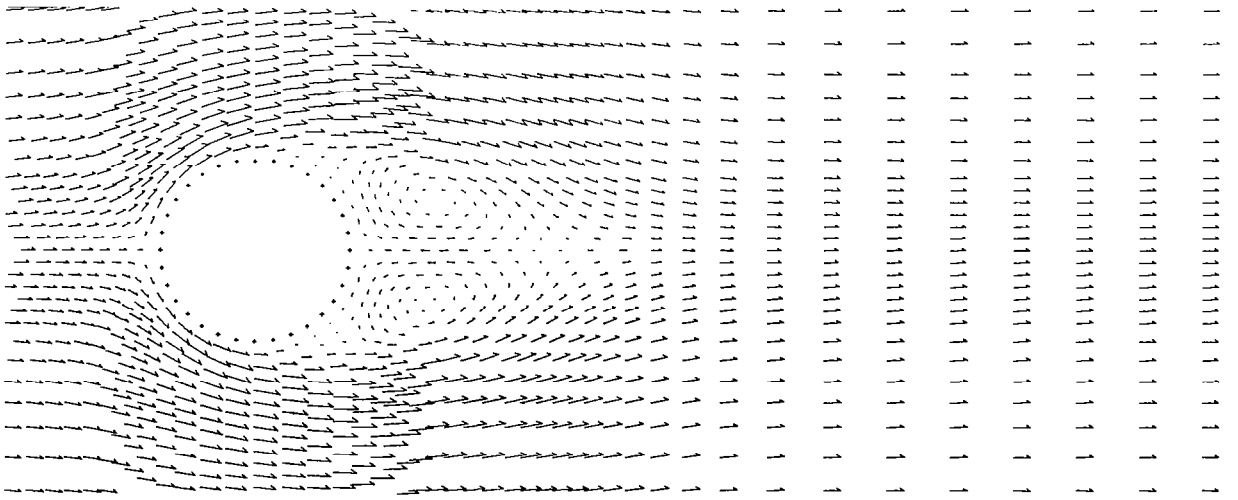

Fig. 21. Problem No. 211.3, R = 100, Medium Mesh; Old boundary condition; Free stream particles have moved 2.38 cylinder diameters.

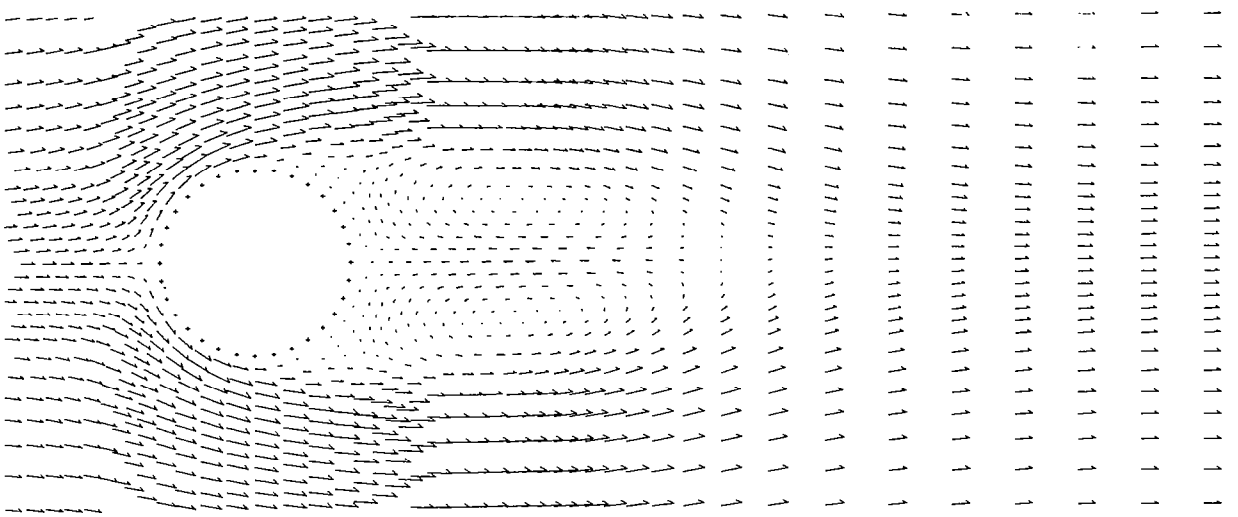

Fig. 22. Problem No. 211.3, R = 100, Medium Mesh; Old boundary condition; Free stream particles have moved 5.12 cylinder diameters.

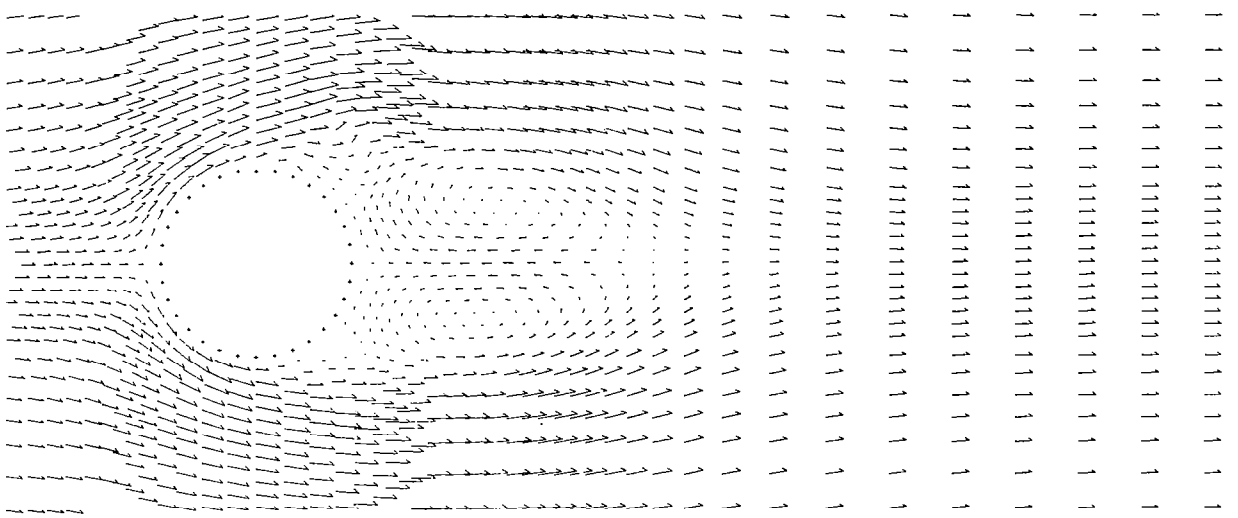

Fig. 23. Problem No. 211.4, R = 100, Medium Mesh; Old boundary condition; Free stream particles have moved 3.89 cylinder diameters.

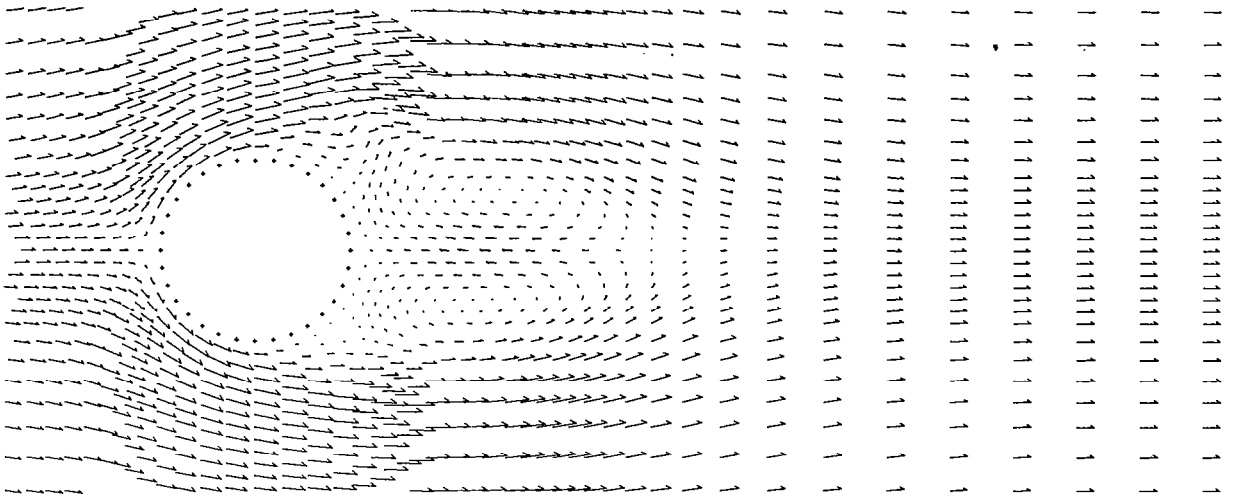

Fig. 24. Problem No. 211.4, R = 100, Medium Mesh; Old boundary condition; Free stream particles have moved 3.97 cylinder diameters.

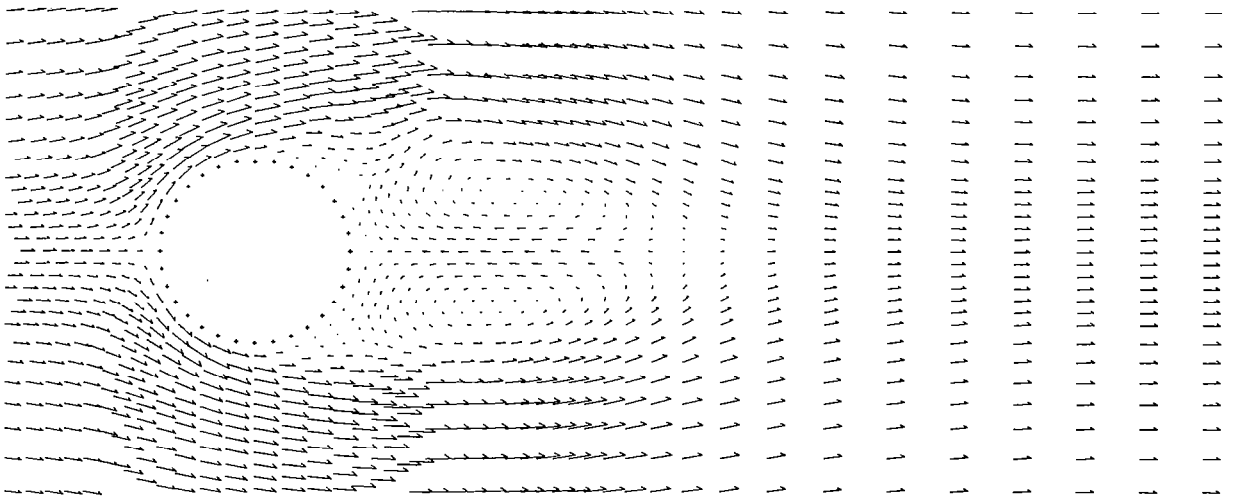

Fig. 25. Problem No. 211.4, R = 100, Medium Mesh; Old boundary condition; Free stream particles have moved 4.36 cylinder diameters.

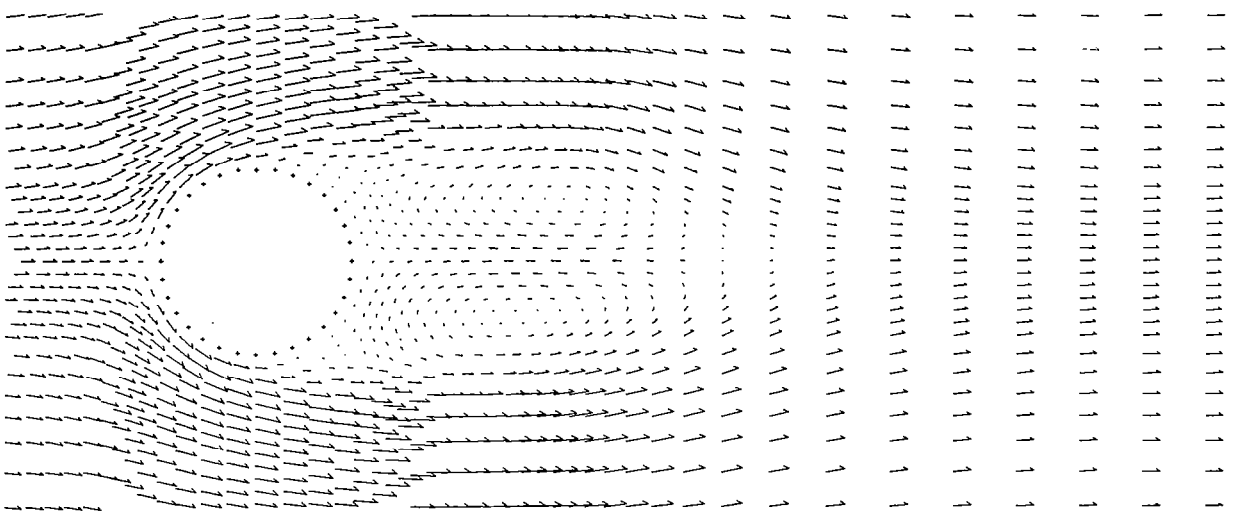

Fig. 26. Problem No. 211.4, R = 100, Medium Mesh; Old boundary condition; Free stream particles have moved 5.16 cylinder diameters.

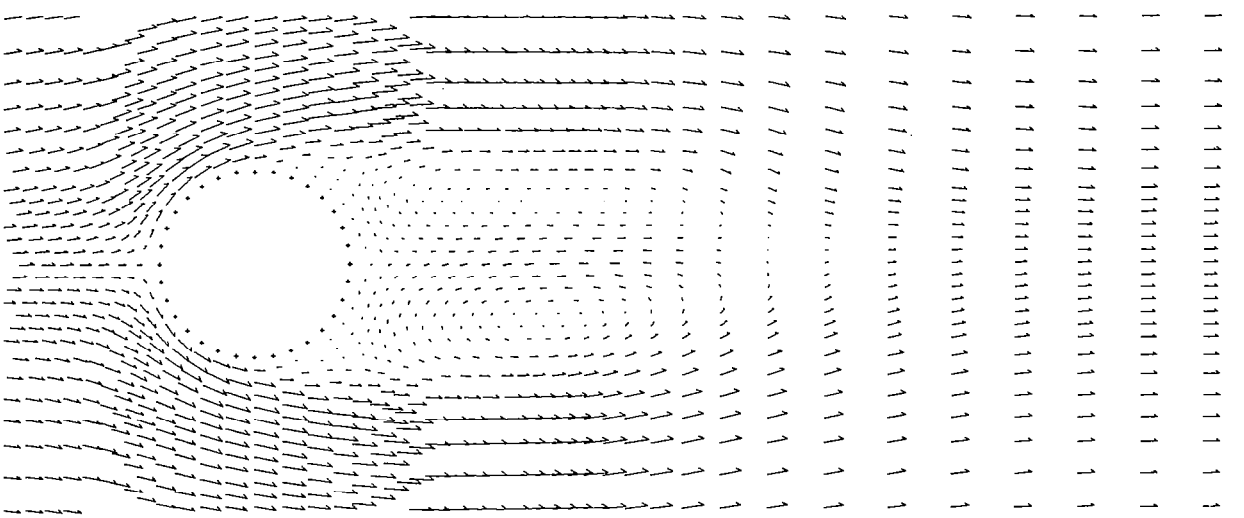

Fig. 27. Problem No. 211.4, R = 100, Medium Mesh; Old boundary condition; Free stream particles have moved 5.95 cylinder diameters.

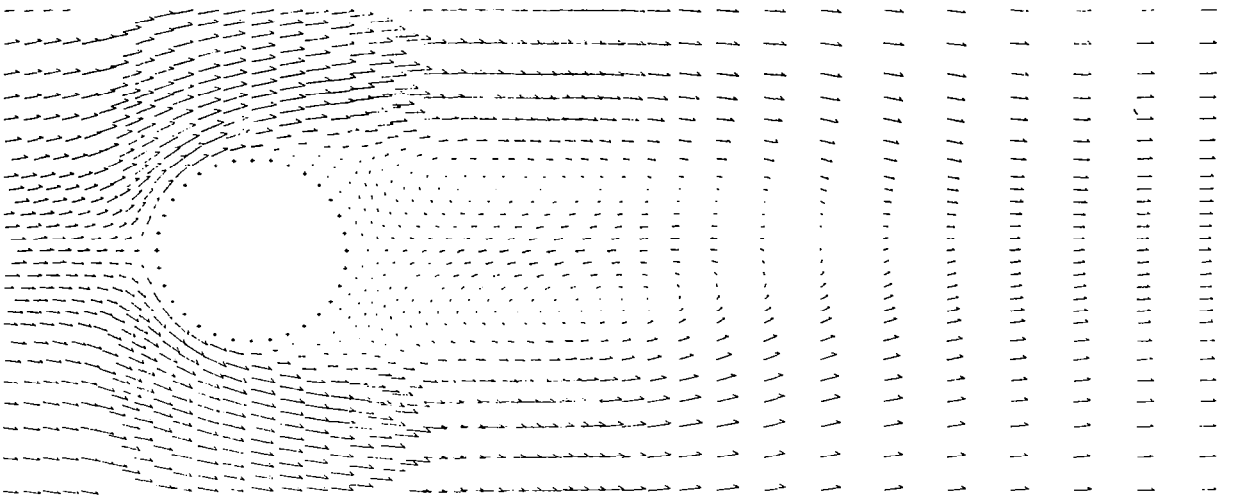

Fig. 28. Problem No. 211.4, R = 100, Medium Mesh; Old boundary condition; Free stream particles have moved 6.74 cylinder diameters.

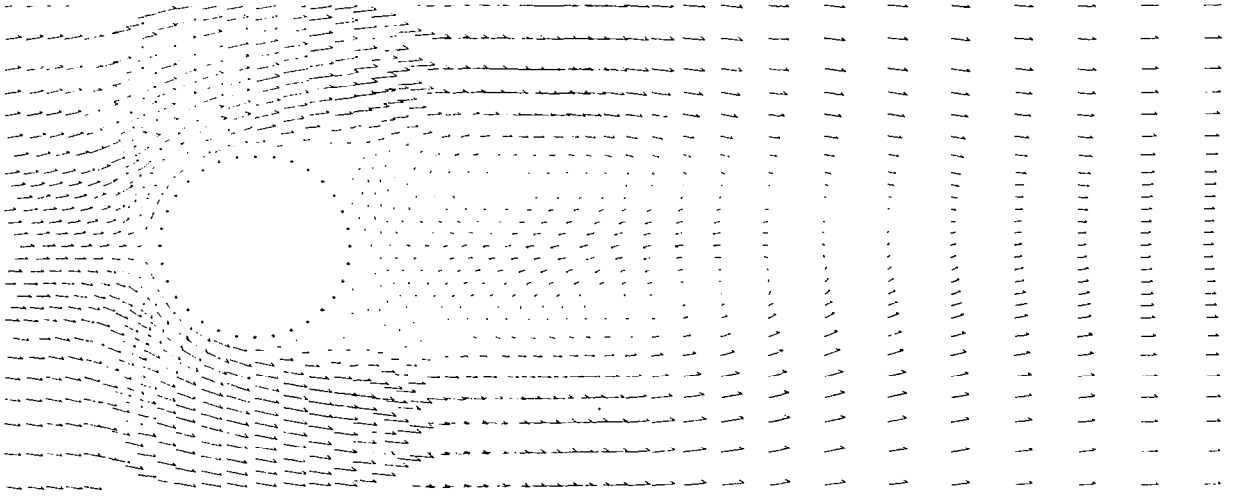

Fig. 29. Problem No. 211.4, R = 100, Medium Mesh; Old boundary condition; Free stream particles have moved 7.54 cylinder diameters.

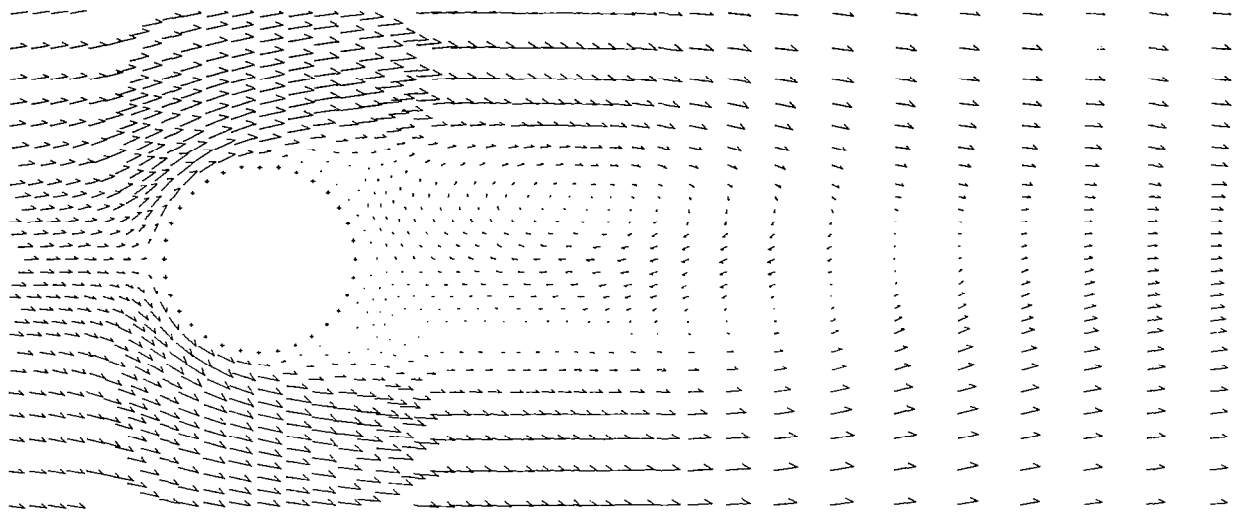

Fig. 30. Problem No. 211.41, R = 100, Medium Mesh; New boundary condition; Free stream particles have moved 8.73 cylinder diameters.

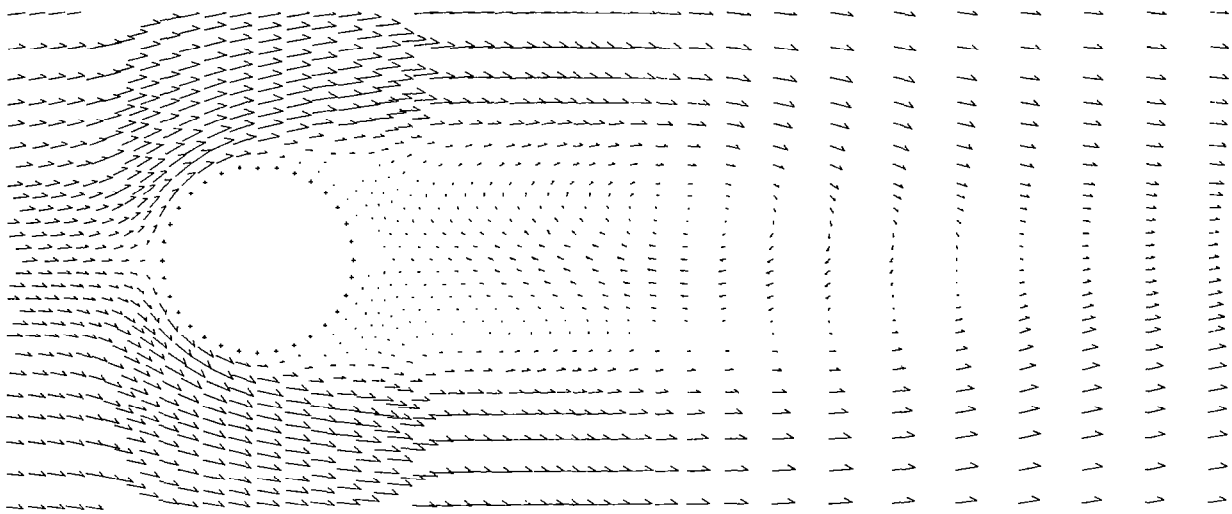

Fig. 31. Problem No. 211.41, R = 100, Medium Mesh; New boundary condition; Free stream particles have moved 9.92 cylinder diameters.

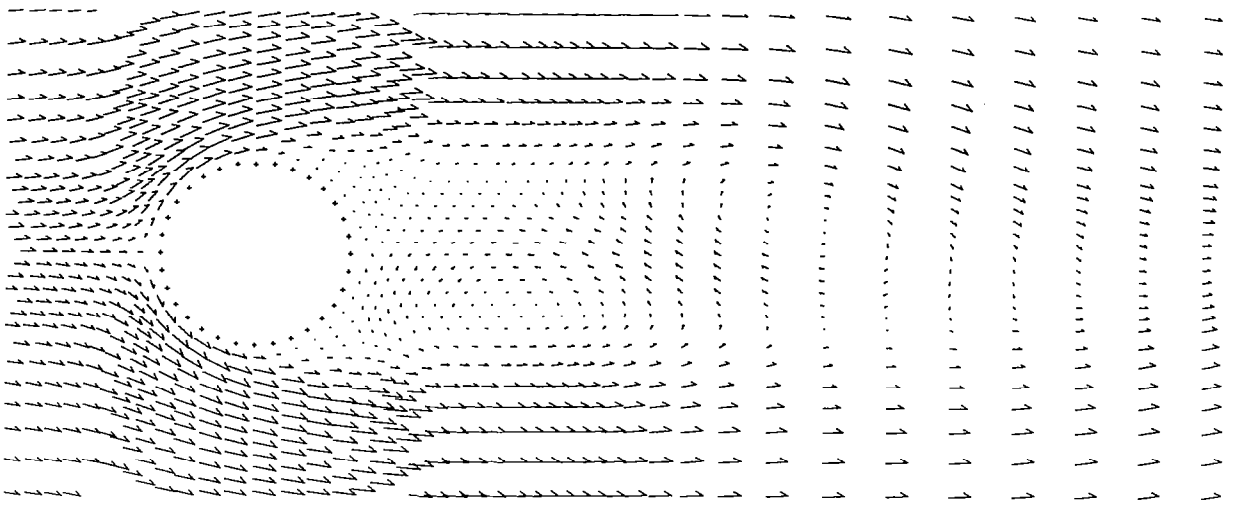

Fig. 32. Problem No. 211.41, R = 100, Medium Mesh; New boundary condition; Free stream particles have moved 11.1 cylinder diameters.

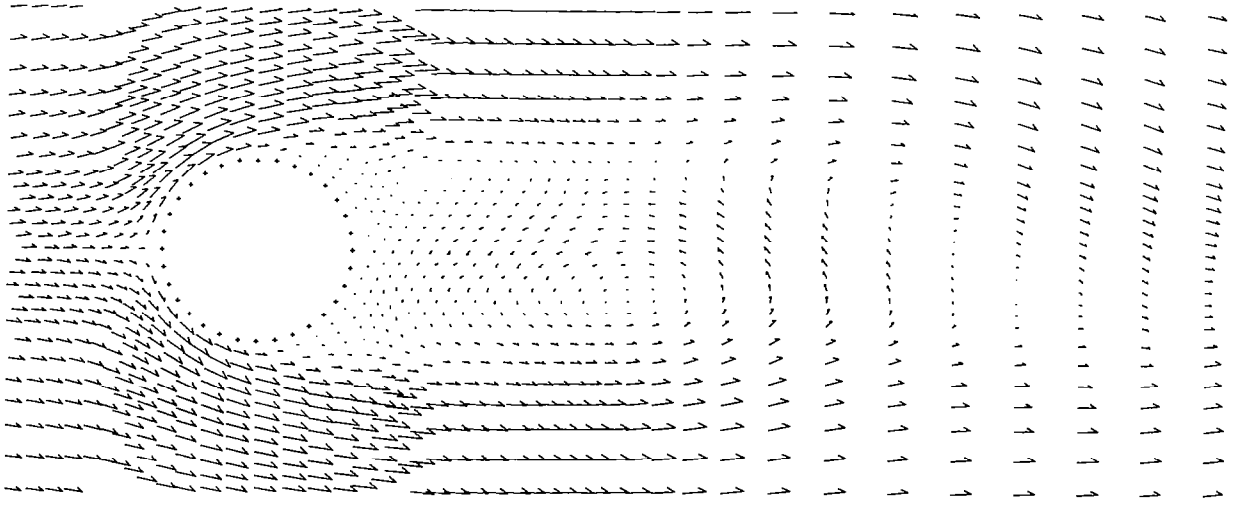

Fig. 33. Problem No. 211.41, R = 100, Medium Mesh; New boundary condition; Free stream particles have moved 12.2 cylinder diameters.

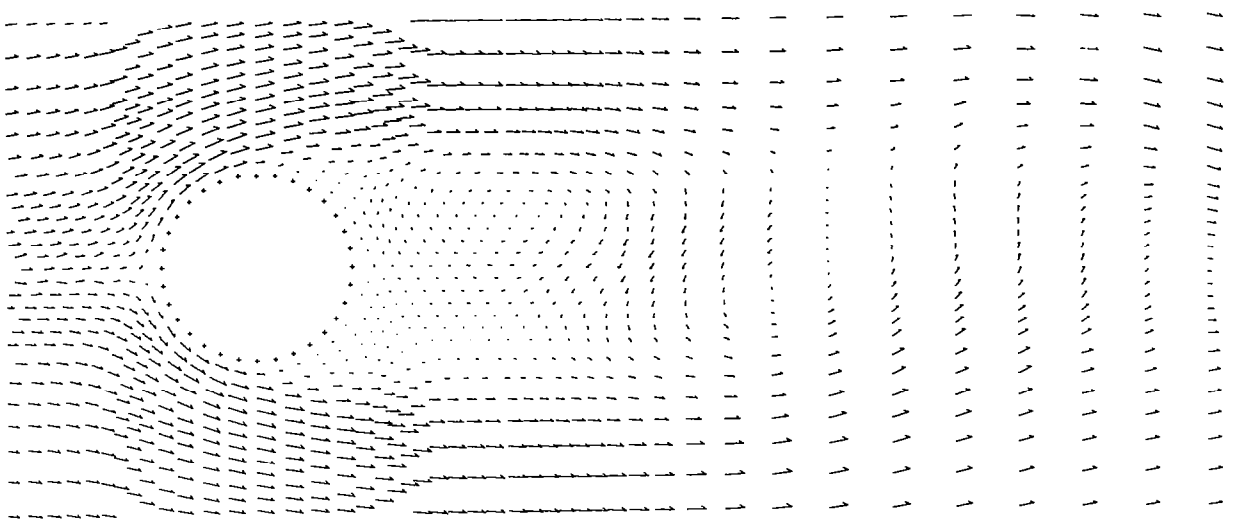

Fig. 34. Problem No. 211.41, R = 100, Medium Mesh, New boundary condition; Free stream particles have moved 13.9 cylinder diameters.

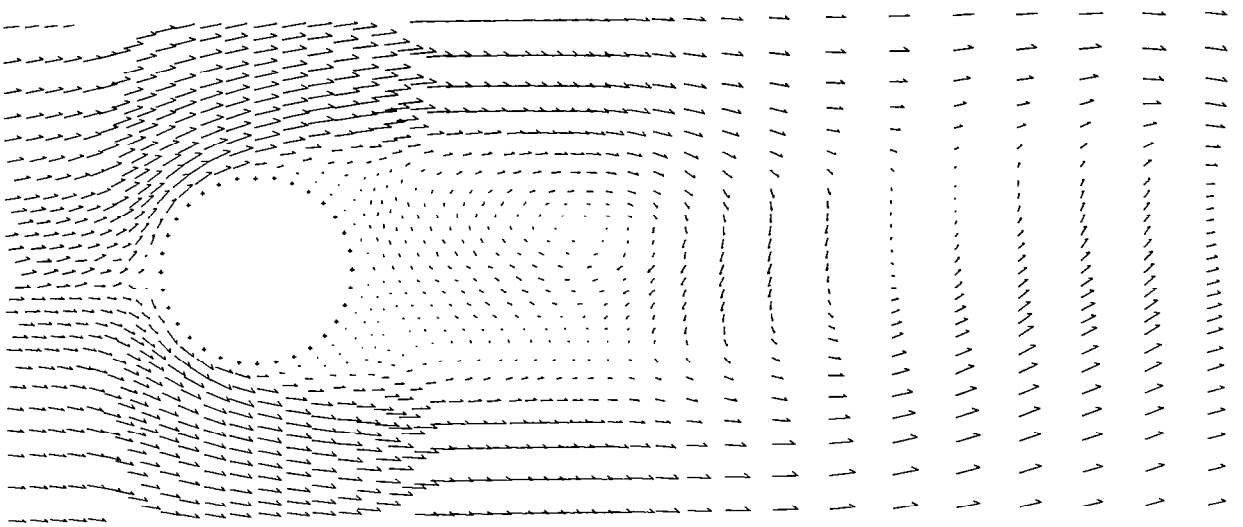

Fig. 35. Problem No. 211.41, R = 100, Medium Mesh, New boundary condition; Free stream particles have moved 14.7 cylinder diameters.

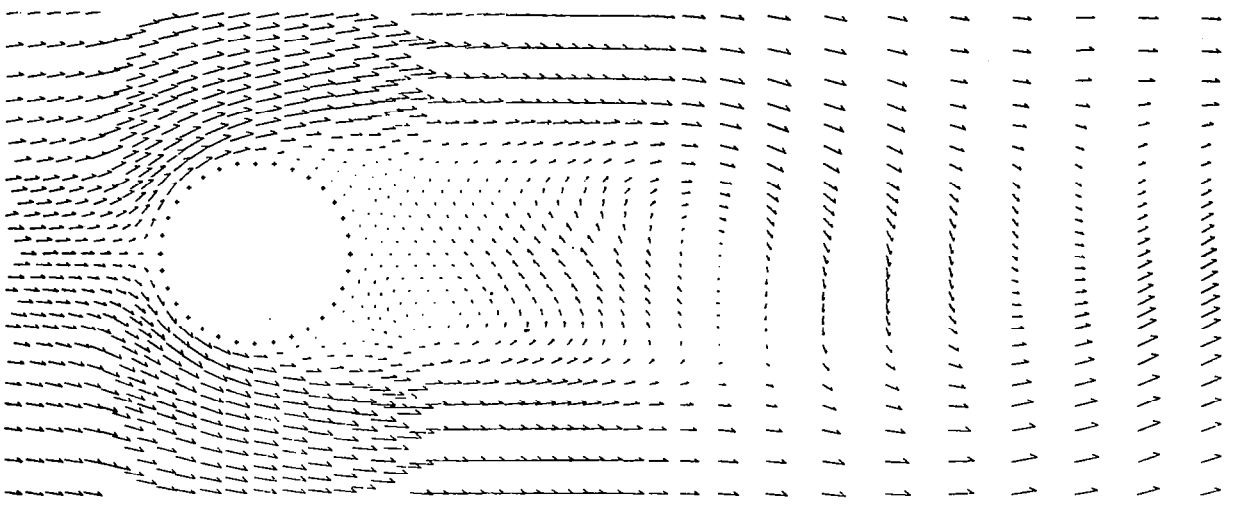

Fig. 36. Problem No. 211.41, R = 100, Medium Mesh; New boundary condition; Free stream particles have moved 15.9 cylinder diameters.

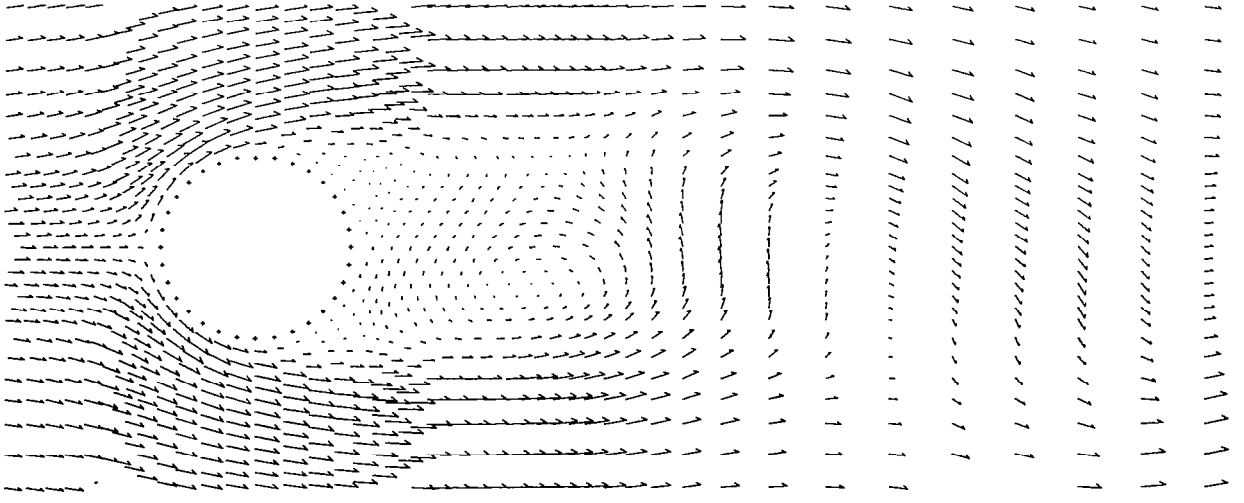

Fig. 37. Problem No. 211.42, R = 100, Medium Mesh; New boundary condition; Free stream particles have moved 17.1 cylinder diameters.

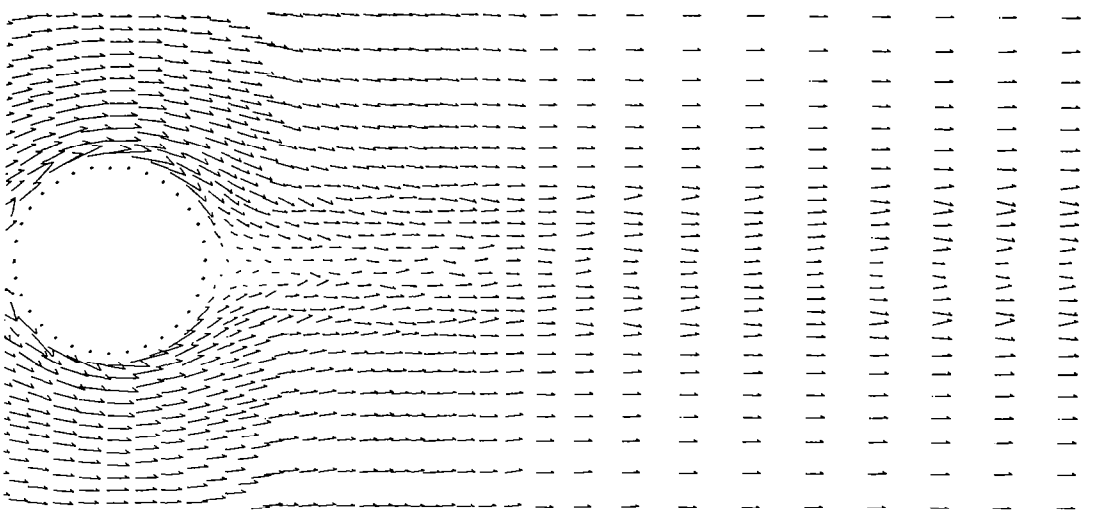

Fig. 38. Problem No. 211.2, R = 5000, Medium Mesh; Free stream particles have moved 4.77 cylinder diameters.

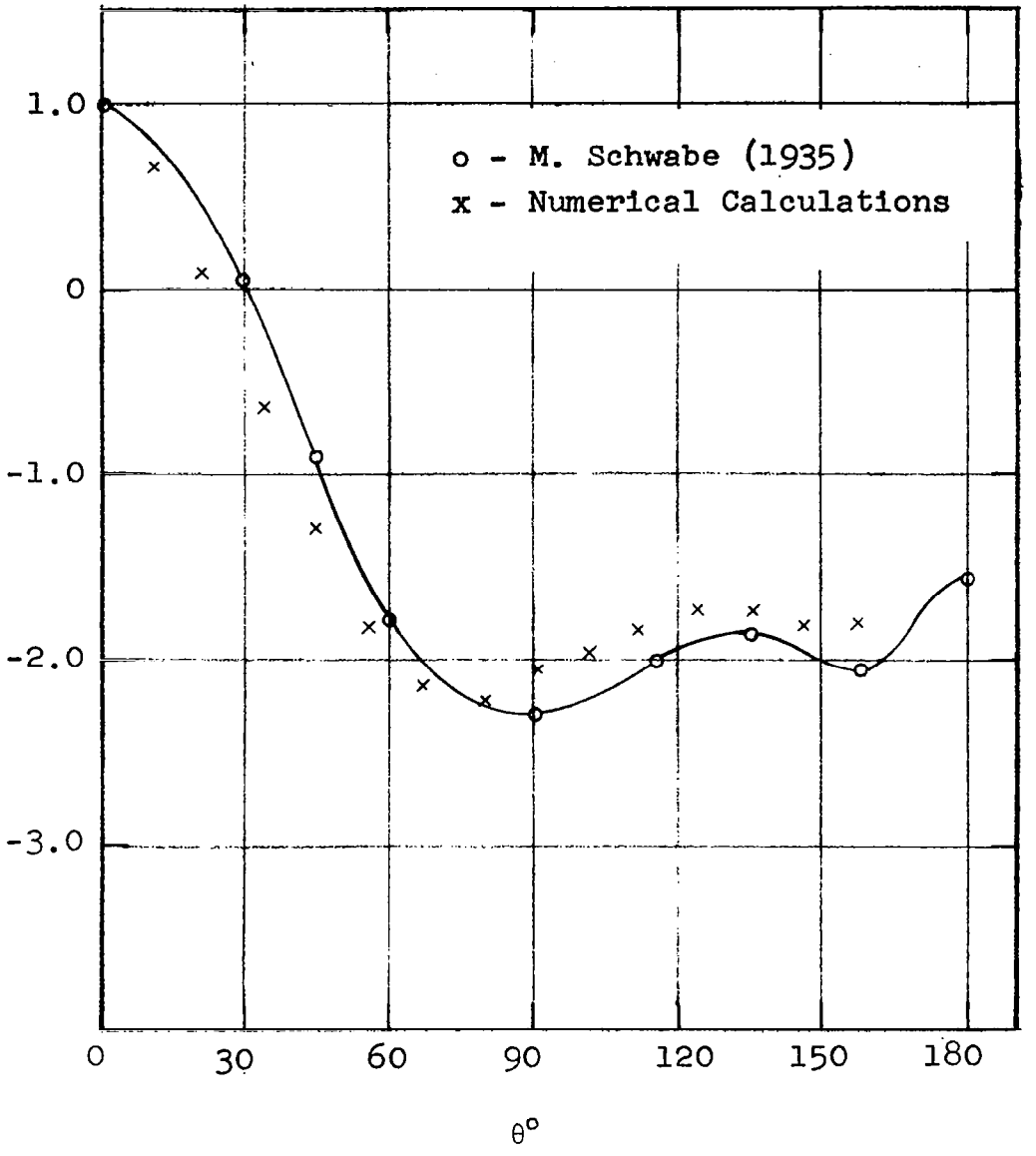

Figure 39

Calculated Pressure Distribution Around a Circular Cylinder During the Starting Process for R = 1000. Medium Mesh Used for the Numerical Calculations.

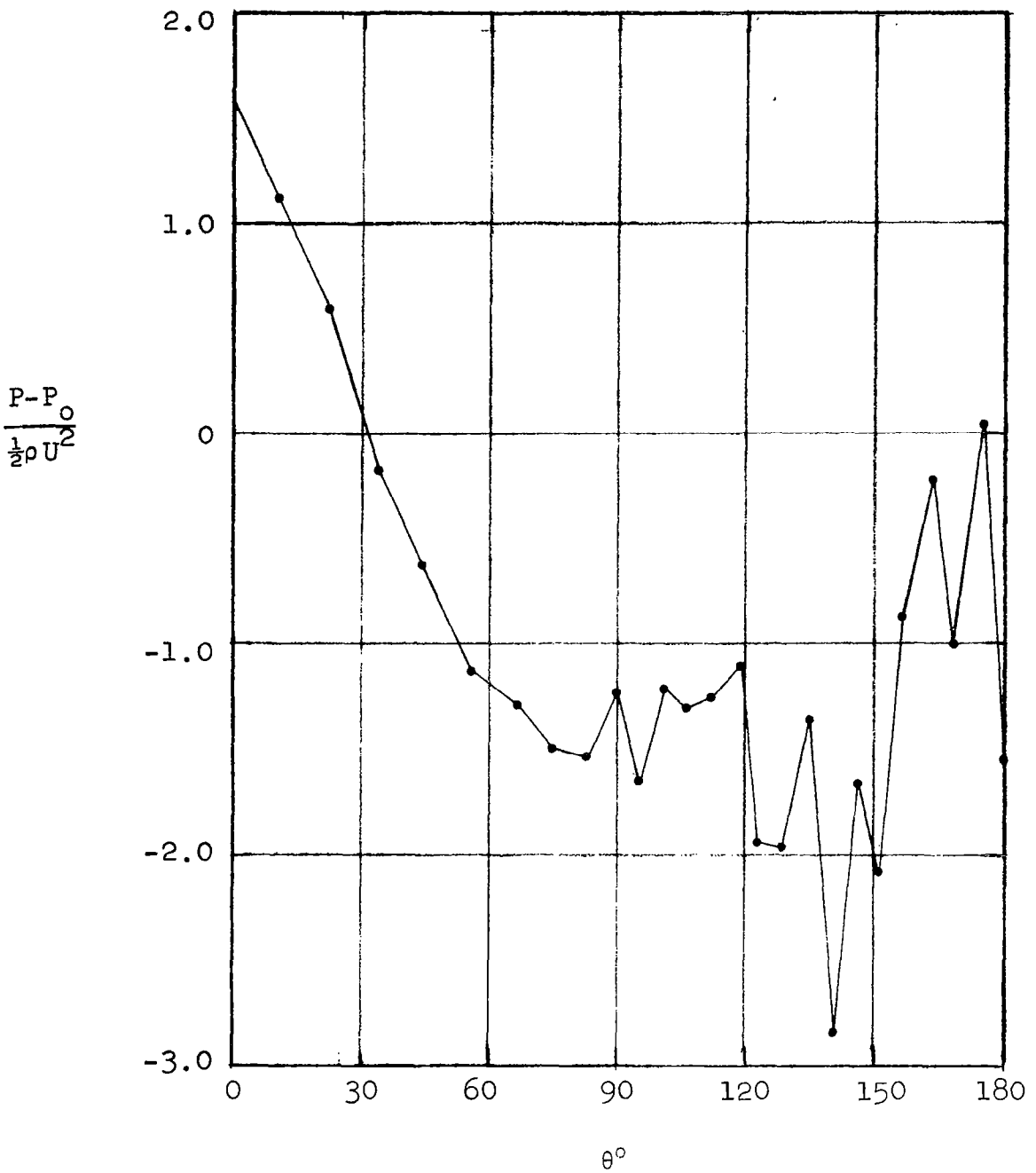

Figure 40

Calculated Pressure Distribution Around a Circular Cylinder During the Starting Process for R = 1000. Fine Mesh Used for the Numerical Calculations.

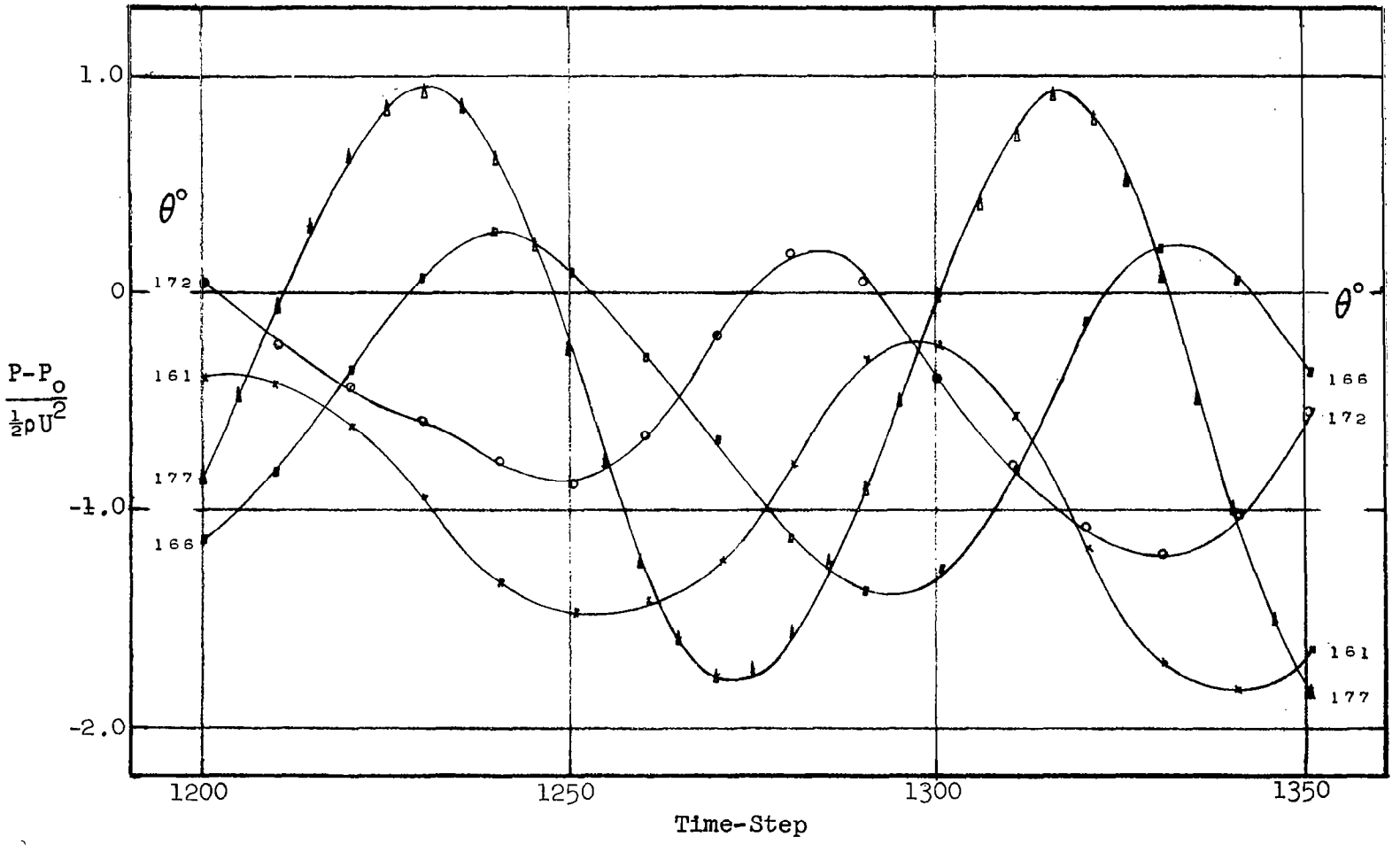

Figure 41

Pressure Variation as a Function of Time-Step for Each of Four Contiguous Zones Located Near the Most Downstream Part of the Cylindrical Surface; R = 1000, Fine Mesh Used for the Numerical Calculations.